

Research papers

The extinguishment mechanisms of a micelle encapsulator F-500 on lithium-ion battery fires

Shuai Yuan^{a,1}, Chongye Chang^{a,1}, Yang Zhou^b, Ruoheng Zhang^a, Jianqi Zhang^a, Yifan Liu^a, Xinming Qian^{a,*}

^a State Key Laboratory of Explosion Science and Technology, Beijing Institute of Technology, Beijing 100081, China

^b Department of Engineering Physics, Tsinghua University, Beijing 100084, China



ARTICLE INFO

Keywords:

Lithium ion battery
Water mist
F-500
Energy safety
Extinguishment mechanism

ABSTRACT

An effective and suitable fire-extinguishing agent used for lithium ion batteries (LIBs) fire currently exists a huge challenge. In this work, extinguishment mechanisms of a micelle encapsulator F-500 were proposed through a series of tests. To clearly understand LIB driven into thermal runaway (TR), gases released from the battery were collected and analyzed. Then, a series of absorption tests were conducted to explore the encapsulator technology of the solution with 3 % F-500. Finally, a series of combustion tests and suppression tests were carried out to verify its suppression effectiveness on LIBs fire. The result indicated that the battery released a great deal of hydrogen and hydrocarbons, which are highly combustible. H₂ and CO account for the largest proportion of these flammable components, which are considered as characteristic gases. Battery module with higher SOC increased difficulty of suppression of TR propagation. The rebounding temperature became higher with increase of SOC when fire-extinguishing agents were applied. 3 % F-500 solution could suppress LIBs fire by combination of absorbing these characteristic gases and excellent cooling capacity. The cooling mechanism of water mist (WM) mainly relied on heat steam. These results are expected to provide a guideline for cooling the LIBs system.

1. Introduction

Compared with other conventional battery, such as lead-acid battery, advanced lead-acid battery, nickel-cadmium battery, zinc bromide flow battery and vanadium redox flow battery, LIBs possess exceptional power density, no memory effect, fast charging ability and long lifespan [1,2]. Nowadays, LIBs have been widely utilized in electronic field, including hybrid electric vehicles (HEVs) or fully electric vehicles (EVs), energy storage system (ESS), aerospace and mobile phone. However, LIBs often goes into TR under condition of abuse, such as acupuncture [3,4], seawater immersion [5], external heating [6–8], overcharge [9,10], which might further triggers fire or even explosion accident. The safety issue of LIB has become the main obstacle to its large-scale application. To improve battery safety, adequate researches have been performed by developing the safer materials such as fire-retardant electrolytes [11–14] and fire-retardant separator [15–18], safer devices such as safety vents [19], external security device such as battery management system (BMS) [20], positive temperature coefficient (PTC)

[21,22], current interrupt device [19,23], and phase change material [24–27]. Nevertheless, the number of LIBs EV fire accident is not obviously reduced in China due to increase in number of vehicles, as shown in Fig. 1. As the increase in the energy density of battery pack, the fire prevention and control strategies of LIBs will encounter bigger challenge. Combustion could occur in the presence of combustible materials, oxygen, and heat sources. Battery possesses many combustible materials including anode material, organic electrolyte and aluminum shell. Oxygen could be release by the decomposition of cathode material [28,29]. The heat can be generated external heat [6–8] and released from exothermic reaction of electrolytes [30]. If only one of these conditions was removed, the fire would not start. Corresponding extinguishment mechanisms include isolation effect, smoothing effect and cooling effect. Therefore, fire suppression technology, as a last defense line, is also essential to improve the safety of battery system and reduce the fire hazard [31].

The thermal runaway behavior of LIBs can be divided into the following stages. The first is the rupture of the battery separator. The

* Corresponding author.

E-mail address: qsemon@bit.edu.cn (X. Qian).

¹ These authors contributed equally: Shuai Yuan, Chongye Chang.

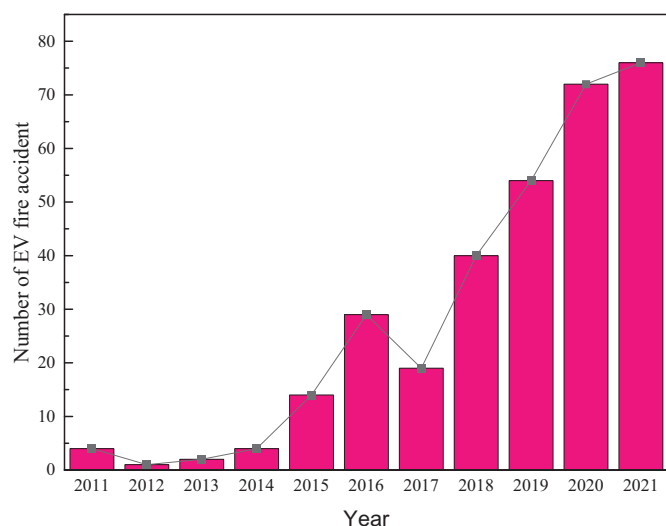


Fig. 1. Statistic of EV fire accidents in current ten years, in China.

separator is damaged due to external impact and battery aging, or the formation of lithium dendrite due to overcharging and low temperature, which pierces the separator [32,33]. The rupture of the diaphragm caused a short circuit in the battery. Then this short-circuiting causes the battery internal temperature to quickly climb up. As the temperature increases, the components of solid electrolyte interphase (SEI) firstly decompose at ~ 100 °C, causing the organic solvents inside the electrolyte to occur reaction with the lithium metal or lithiated carbonaceous anodes [34,35]. These exothermic reactions cause the battery temperature to rise, and more and more gas is generated inside the battery until it breaks through the safety valve [36]. The separator would melt at around 130 °C, triggering further exothermal reactions between positive electrode and negative electrode [37–39]. The ejection with sparks occurs when enough oxygen and heat are accumulated. These sparks might be the result of combustion of aluminum particles and electrode fragments [40]. Subsequently, the thermal runaway occurs from a location to the whole battery [41]. A jet fire subsequently happens above the battery safety valve due to the spray of flammable gases and volatile electrolytes [42]. Eventually, the battery undergoes a stable combustion stage, then weakening to extinguishment.

As mentioned about understanding of the mechanism of LIBs thermal runaway, the key characteristics of LIBs fire can be summarized as follows: 1) it takes merely several seconds for the temperature to rise up to the maximum temperature of thermal runaway. And the maximum temperature of a LIBs is very high. 2) LIBs fire will release a large number of flammable, explosive and toxic gases, which is prone to secondary accidents. 3) LIBs fire extinguishing not only needs to extinguish the open fire, but also needs rapid cooling effect.

To eliminate the fire hazards, the efficiency of various fire extinguishing agents has been conducted. Researchers explored the efficiency of dry powder on suppressing LIBs fires [43–38]. Experimental results showed that dry powder could put out LIBs fire, but it has little effect on reducing the peak temperature of LIBs [43,44,48]. Re-ignition easily happened after the release of dry powder was suspended because ABC dry powder possesses a low specific heat capacity (~ 1.29 kJ/kg \cdot °C) [45,47]. As a replacement of halons, carbon dioxide (CO₂) has been used in many fields owing to its insulation [49]. The extinguishment efficiency of CO₂ is associated with a combination of the reduction of oxygen and combustible vapor concentration and endothermic reaction [50–52]. Some scholars explored the suppression of CO₂ for LIBs fire [44,47,53–56]. The results indicated that CO₂ cannot put out the LIBs fire [44,54,56] and re-ignition often happens [47,53,55] due to its low thermal conductivity (0.016 W/m/K) and poor specific capacity (0.85 kJ/kg \cdot °C). A CO₂ extinguisher releases a two-phase mixture meant to

O₂-starve the flame. C₃F₇H is also one of replacement of halons, which suppress fire mainly rely on absorbing heat and diluting oxygen. Compared with CO₂, C₃F₇H possesses higher thermal conductivity (0.069 W/m/K) and better specific capacity (0.94 kJ/kg \cdot °C). Previous studies indicated that C₃F₇H could put out lithium titanate (LTO) battery fire within several seconds [57]. However, the battery still re-burned during the spraying of C₃F₇H [53,56]. In 2001, C₆F₁₂O was produced by 3 M, which has been used in many field due to its nearly zero ozone depletion potential, global warming potential (GWP) of 1 and atmospheric lifetime (ATL) of 0.014 [58]. The agent extinguishes the flame though absorbing heat due to its high heat of vaporization at boiling point (88 kJ/kg) [59]. On this basis, the clean agent has been used to extinguish LIBs fire. For instance, Wang et al. found that Novec 1230 could extinguish LTO battery fire within 30 s, while the clean agent needed continuous spraying to prevent re-ignition of battery [60,61]. Meanwhile, the agent showed an ideal fire prevent effect when battery was immersed in Novec 1230 [62]. In addition, the dose and flow rate of fire-extinguishing agents has a dramatic effect on extinguishing LIBs fire. For example, experimental research conducted by Wang et al. indicated that a low dose of Novec 1230 might increase the maximum temperature of LIBs [61]. They suggested that the suitable does of Novec 1230 was 9.42 g/Wh for a 38 Ah Li(Ni_{1/3}Co_{1/3}Mn_{1/3})O₂ battery in given condition. Continue spraying at an adequately high flow rate with this agent is conducive to suppressing open flame of lithium cobalt oxide (LCO) battery module but not completely prevent TR propagation [59]. In all, gaseous fire-extinguishing agents could put out open flame, but could not rapidly cool the battery during TR, which cause the re-ignition of battery.

Water possesses excellent cooling ability due to its specific capacity (4.12 kJ/kg \cdot °C) and great latent heat of vaporization (~ 2266 kJ/kg/K). Water spray technology refers to the technology that sprays the liquid under a certain pressure to make the diameter of 99 % of the droplet volume ($dv_{0.99}$) < 1000 μ m [60]. Water spray technology is used in many fire protection fields due to no toxic, low electric conduction and less consumption. Recently, Wang and his team [64] provided a novel strategy that combing Novec 1230 with water mist (WM, water ejected using water spray technology) used for suppressing LIBs fire. The combination method showed excellent effects of suppressing open fire and cooling battery. The results showed that reduction in the maximum temperature of battery was 117 °C when the combination was applied, while the reductions were 75 and 19 °C when only water mist only or Novec 1230 only was applied, respectively. Therefore, excellent cooling ability is same important as rapid extinguishing open fire. Rao et al. [47] compared the effectiveness of different fire-fighting agents (such as dry powder, CO₂ and C₃F₇H) on LFP battery fire. Result indicated that C₃F₇H was the most effective agent on extinguishing flame and cooling the battery. WM mainly suppresses fire by oxygen dilution and high cooling efficiency owing to its greater latent heat of vaporization (~ 2266 kJ/kg/K) [53]. Compared with CO₂, C₃F₇H and C₆F₁₂O, WM exhibited more excellent extinguishing effect and cooling effect for battery underwent TR [53,65].

Currently, some researches have been conducted to try the application of WM for cooling and inhibiting TR of battery. For example, Liu et al. [66,67] explored the inhibition effect of WM on TR of single battery and the prevention effectiveness of TR propagation of battery module. TR of individual battery cannot be inhibited when water mist was sprayed after the threshold temperature of battery. The temperature often was not less 20 °C below the TR onset temperature. Compared with CO₂ (3.38 g/Wh) and phase change material (38.4 g/Wh), the consumption of WM (0.195 g/Wh) is the lightest in propagation prevention of battery module [66]. The cooling capacity and extinguishment effectiveness of water spray on LIB during TR are related to spray parameters such as spray pressure [67], spray duration [68,69], intermittent spray cooling [70] and spray trigger temperature [69]. However, cooling efficiency of WM will encounter a big challenge in some condition, such as LIB modules are connected with parallel method

[71] and overcharge triggers TR of LIB [72]. Russoa et al. [44] found that WM showed less effective on reducing battery temperature and suppressing open fire than water and foam. This is because the amount of water passed through battery flame is fairly limited when water is applied by Water spray technology [1]. Therefore, Water spray technology, as an effective fire extinguishing agent injection method, has been concerned by scholars.

To improve the effectiveness of water, in addition to the use of water spray technology, water containing additives has been concerned on extinguishing LIBs fire. These additives can be divided into physical surfactant [64,73–79], inorganic salt electrolytes [74,75] and compound additive [64,76,77,79–82]. The surfactant changes the physical characteristics of water such as reducing the surface tension of pure water, which further decreases particle size and permeability of water. Inorganic salt electrolytes suppress fire by quenching [H] and [OH] and suffocation action [64]. Additionally, the previous results showed that compound additives could extinguish LIB fire within 2 s and its corresponding cooling rate is 0.755 °C/s, while single additive could suppress the fire at least 4 s and corresponding cooling rate is 0.62 °C/s [83]. Some experimental results indicated inorganic salt electrolytes with WM shows a more advantage in preventing the temperature rise of LIBs than surfactant with WM [83]. Surprisingly, some experimental results indicated that adding surfactant into water showed a less effective in reducing the temperature rise and controlling TR propagation in battery-module than WM [64,73]. Even so, compared with gaseous extinguishing agents, water-based extinguishing agents have more advantages in cooling capacity and prevention re-ignition of battery module [84]. Nowadays, F-500 additive is an effectiveness agent regarding LIBs fire [79]. It is not always the best idea to extinguish a Li-ion battery fire. If extinguished, the batteries will continue to release unreacted gas that may form a reactive cloud with air. It is an important argument for using micelle encapsulators. However, its extinguishment mechanisms by water spray technology for LIBs fire have never been reported.

In this paper, a series of experimental researches were conducted to deeply investigate the extinguishment mechanisms of a micelle encapsulator F-500 on LIBs fire. According to the use guide published by F-500 development company (Hazard Control Technologies, Inc.), the solution with concentration of 3 % is selected as the experimental object. Firstly, the released gases of cells at various state of charges (SOCs) were taken and analyzed. Then, the gases absorption tests were conducted to explore encapsulating gas capacity of 3 % F-500 solution. Meanwhile, absorption state was characterized by dynamic laser light scattering (DLS). Combined with the measurement of surface tension, viscosity, it could be concluded that lower surface tension and suitable viscosity were conducive to cool the battery modules. The findings provided here could shed light on further improving the extinguishing efficiencies of new agents for suppressing LIBs fire.

2. Experimental

2.1. LIB

This paper used 18,650-type cylindrical LIB with a capacity of 3 Ah and a nominal cell voltage of 4.2 V. The cathode and anode materials contain NCA(LiNi_{0.8}Co_{0.15}Al_{0.05}O₂) and graphite respectively. The mass of cell removed the plastic packaging is 46.8 ± 0.20 g. The battery has two safety valves, located in upper and bottom, respectively. A NEWARE CT-4008 T battery testing system was used to prepare the cells tested. According to the steps, the LIBs were first laid aside 2 min, then discharged with a constant current 1.7 A to 3 V, and the laid aside 2 min. Then LIBs were full charged to 4.2 V with the constant current/constant voltage until the charge current fell below 34 mA. Finally, the LIBs were packed to the desired SOC with a constant discharge current of 1.7 A. Hereafter, the cells were standing for 4 h to ensure the stable performance of battery before tests.

2.2. Experimental process

2.2.1. Characteristic gases of battery test

The TR of battery was conducted in a sealed tank, as showed in Fig. 2. The container was cylindrical tank of 250 mm (Inner diameter) × 300 mm (Height) × 100 mm (Thickness), which was made of the stainless-steel material. The tank was equipped with a gas filling system, an exhaust valve, a vacuum pump, a gas collection valve and a digital pressure gauge. A gas sampling valve was used to collect the gases generated from TR happened in the battery. The pressure inside the tank was recorded by a pressure transmitter. Two thermocouples were used to monitor the temperatures inside the tank environment and battery surface, respectively. Before the experiment, the vacuum pump was opened to draw out the air inside the tank and fill it with a certain amount of helium to ensure the value of pressure inside the tank is 0.1 MPa, which was operated for more than three times to ensure that the tank filled with helium gas. Then stand for 10 min to ensure that the temperature of the sealed tank is the same as the external ambient temperature. At the beginning of the experiment, the electric heating system was turned on and the electric heater was heated at a rate of 10 °C/min. When temperature of battery increased several hundred °C in a matter of seconds, the tested battery was identified as TR, then battery cools down slowly [85]. To repeat the experiments, the heater was shut down after surface temperature of tested battery reached the maximum temperature. This is because the battery is under the stage of cooling down slowly. During this process, the temperature and pressure inside the container was collected by the paperless recorder. The released gases were collected by a high temperature air collecting bag. Then, the compositions of the gases were analyzed by using gas chromatography and mass spectrometry (GCMS, SHIMADZU GCMS-TQ8040NX). The MS was used to detect TR gases. The GC was calibrated for H₂, CO₂, CO, CH₄ and C₂H₄. The carrier gas is the helium gas. In order to ensure that there are no other interference factors, this paper makes a series of blank experiments without battery for comparison. On the premise of the same experimental conditions, the electric heater was heated to 100 °C, 200 °C, 300 °C and 400 °C respectively according to the same heating rate (10 °C/min). Then the gas was collected and analyzed by GCMS.

2.2.2. Gases absorption test

To explore whether the 3 % F-500 solution could absorb the characteristic gas (H₂ or CO) or not, a preparation facility for standard gas samples was established, as shown in Fig. 3. Firstly, to prepare the gas-saturated solution, the characteristic gas of the battery was pumped into a 1000 ml conical flask filled with 3 % F-500 solution for 30 min. Then, the micelles size of the solution after the gases absorption tests was investigated by dynamic laser light scattering (DLS). If 3 % F-500 solution could absorb the characteristic gases, the micelles size of solution got from gases absorption test will bigger than before.

2.2.3. Viscosity and surface tension test

The water-based fire-extinguishing agent is transported to the nozzle through the pump. Hence liquidity is an important parameter in this work and viscosity is another significant parameter to affect the liquidity and evaluate the injection way. High-viscosity fire-extinguishing agent is incapable of releasing through nozzle and penetrating into the battery module. Therefore, viscosity and surface tension were measured by a digital rotary viscometer (NDJ-8 s) and BZY-101 series automatic surface tensiometer, respectively.

2.2.4. Fire extinguishing test

The arrangement and number of the battery modules can have an enormous impact on the effectiveness of fire extinguishing. Fig. 4 exhibits the configuration of battery module and arrangement of thermocouples. As showed in Fig. 4(a), the used cell module was arranged in a rectangular array (as a kind of common array in ESSs) without spacing.

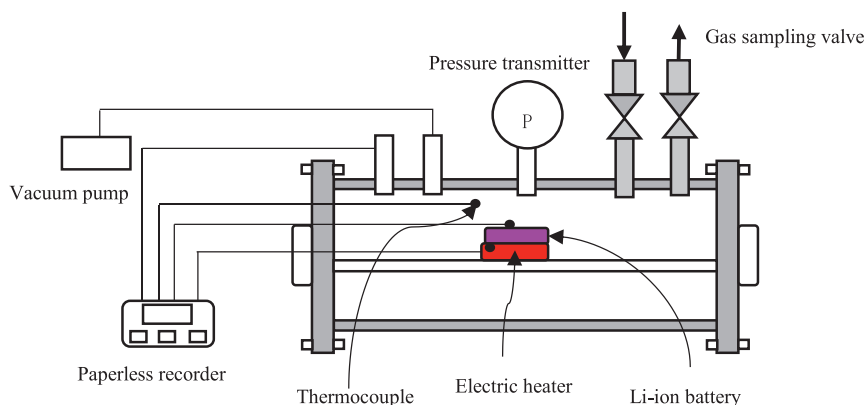


Fig. 2. Schematic diagram of TR gas collection device.

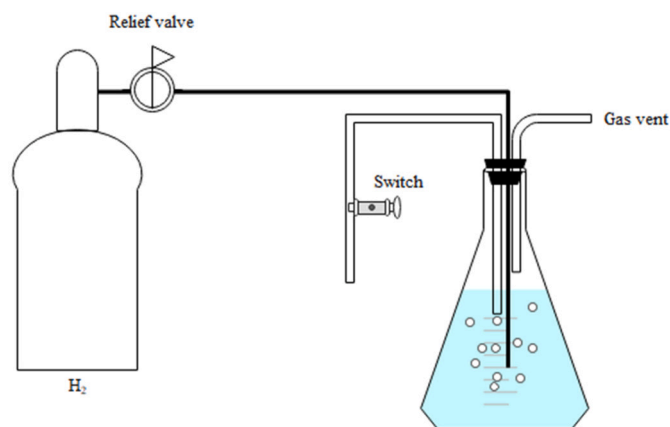


Fig. 3. Schematic diagram of gas absorption device.

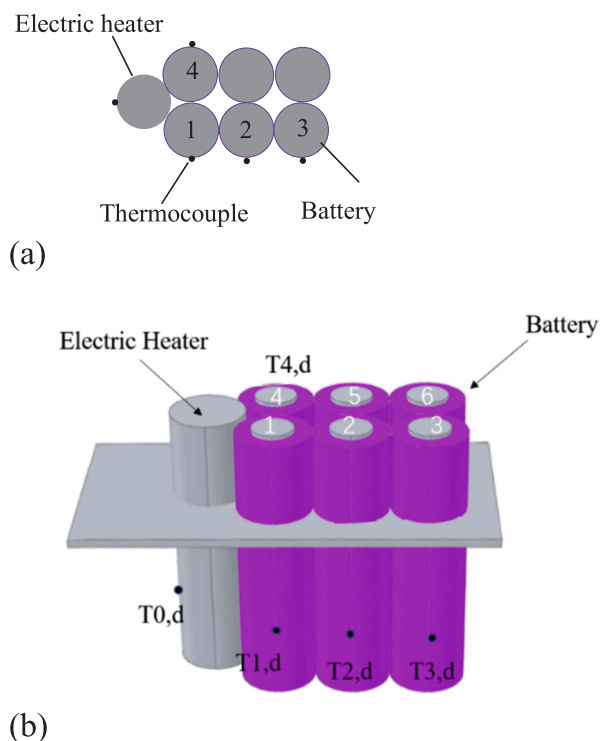


Fig. 4. (a) Distribution of the tested battery modules and (b) 3D rendering of the battery holder.

Two nickel-chromium wire (0.7 mm thickness) and the rectangle stainless steel battery holder were used to fasten the battery module and prevent battery from fleeing during TR, as shown in Fig. 4(b). The gray cylinder (18 mm in diameter, 130 mm long) represents a 350 W electric heater, used for initiating TR of battery tested. One K-type thermocouple was attached to the heater to control the temperature rising rate ($10\text{ }^{\circ}\text{C}/\text{min}$) of the heater by single chip. The maximum temperature on the heater was set for $330\text{ }^{\circ}\text{C}$. Based on practical engineering applications, not all cells need to be arranged with the thermocouples. In our work, we mainly focused on the battery #1-#4 due to their symmetric arrangement, as shown in Fig. 4(a). The temperatures mentioned above during process of experiment were monitored and recorded with a THM167 data acquisition at a frequency of 1 Hz.

Fig. 5 shows a schematic diagram of the combustion and suppression test apparatus used in the paper. The apparatus mainly consists of a combustion chamber, a high-pressure water spray system, an exhaust system, external heat system, thermocouple data loggers and digital video camera. The apparatus was a cuboid of 700 mm (width) \times 1015 mm (length) \times 1820 mm (height), which was made of 304 stainless steel. A digital video camera was used to observe the experimental phenomenon through explosion-proof glass window. To effectively extinguish the battery fire, high-pressure WM atomizer nozzle was placed directly above the battery. To reduce the error brought extinguishing agent or water transport in the fire extinguishing pipe, solenoid valve was installed near nozzle. The fire-extinguishing agent was collected by a waste liquid dish after the suppressing experiment. So at least three groups of experiments are done in each group to ensure the reliability of data.

The paper mainly explored the extinguishing effectiveness of F-500 by suppressing tests. The SOCs, various fire-extinguishing agents in this work are listed in Table 1. For test group 1–6, free-burn tests and pure WM tests were conducted to provide a benchmark. Considering that it took a certain of time for agents to spray from the nozzle, pump was turned on for 1 min to ensure agents filled the extinguishing pipe before suppressing tests. The electric heater was immediately turned off and pump was opened after fire occurred in the first battery. The duration of agents released was 30 s and volume of agent released was $0.81 \pm 0.1\text{ L}$ in this paper. For test group 4–9, the distance between the nozzle and the battery was approximately 46 cm. The working pressure of WM (P) was fixed at 5.5 MPa. The flow of nozzle (Q) was 1.62 L/min and its spray angle of agent was 60° . The flow discharge coefficient can be figured out by following Eq. (1):

$$Q = K\sqrt{10P} \quad (1)$$

where K is the flow discharge coefficient. Table 2 summarizes the detail characteristics of WM.

The surface temperatures of batteries were recorded by thermocouples during the tests. To ensure the accuracy of experiment, all the tests

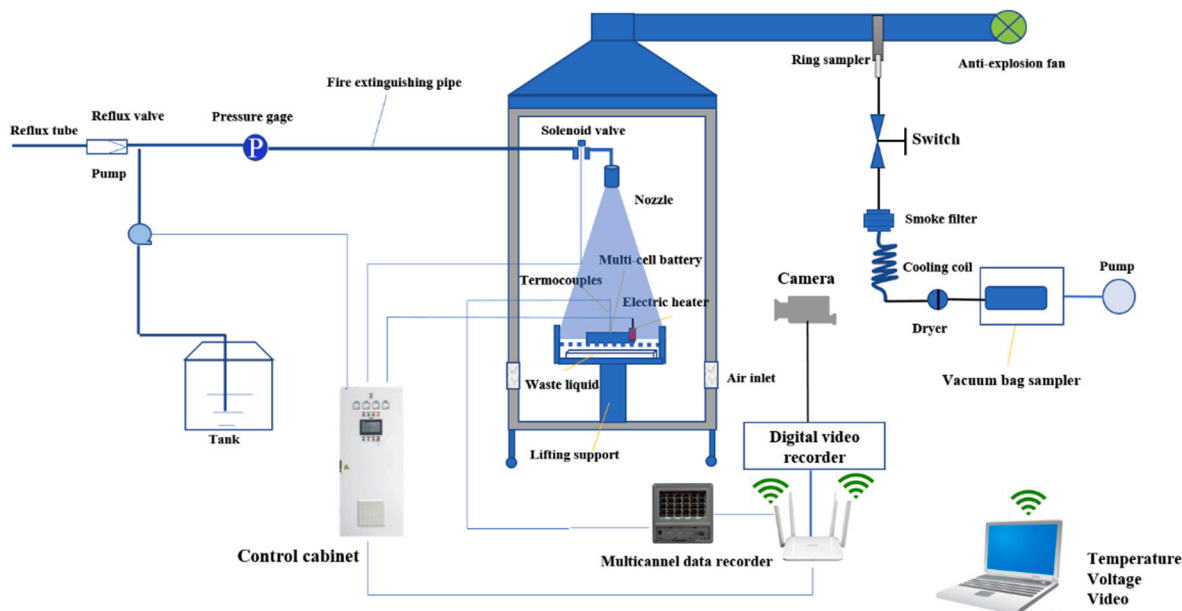


Fig. 5. Schematic of experimental apparatus.

Table 1

Experimental conditions for tests.

No.	SOC/ %	Agents	Moment of release	Pressure/ Mpa	Duration/ s	Volume/ L
1-3	60/ 80/ 100	/	/	/	/	/
4-6	60/ 80/ 100	WM	The first battery occurs jet fire	5.5	30	0.81
7-9	60/ 80/ 100	3 % F- 500 solution	The first battery occurs jet fire	5.5	30	0.82

Table 2

Characteristics of WM.

Nozzle working pressure (MPa)	Flow rate (L/min)	Flow discharge coefficient ($L \cdot \text{min}^{-1} \cdot \text{MPa}^{-0.5}$)	Cone angle ($^{\circ}\text{C}$)
5.5	1.62	0.22	60

mentioned above were repeated at least twice.

3. Results and discussion

3.1. TR propagation under different SOC

Fig. 6 presents the surface temperature of battery modules with different SOC during TR propagation. TR generally occurs when the heat produced by exothermic reactions in battery overpasses heat consumption to the environment [19]. The temperature will gradually increase with the aggravation of exothermic reactions among components in the battery. When the temperature increases at an exponential rate, the TR occurs. Hence, the TR onset temperature (T_r) of battery is one of significant parameters. In our study, the critical temperature was chosen as T_r when the rate of temperature rise reached $10\text{ }^{\circ}\text{C/s}$. As Fig. 6(a-c) shows, battery module with three kinds of SOC happened a similar TR propagation process (#1 \rightarrow #4 \rightarrow #2 \rightarrow #3). In other words, battery modules could happen TR phenomenon from one row to the next. The

surface temperature of battery increased gradually with the continuous heating. The temperature curves of battery #1 and battery #4 are almost overlapping owing to their symmetric arrangement. The temperature of batteries in the module become low from left to right. TR initiated in battery #1 and battery #4 at the early of stage due to their direct contact with the heater. The battery #1 and battery #4 were expected to initiate TR at the same moment due to their symmetric arrangement. However, the battery #1 firstly experienced TR, and propagated battery #4, owing to manufacturing difference of battery. The electric heater was turn off when the first battery experienced fire. Hence, following TR propagation relied on the heat produced inside the first battery.

Table 3 presents some significant parameters of the TR propagation with different SOC. The maximum temperature (T_{max}) during the TR process indicates the maximum heat produced inside the battery. The battery #1 and battery #4 represent the batteries of first row in the module. The battery #2 represents the battery of middle row in the battery module. The battery #3 represents the battery of last row in the module. As shown in Table 3, the batteries in the middle row encountered serious heat hazard process with the highest temperature when the SOC of battery module was 60%. This is because the TR happened in the batteries of the first row by the not high temperature of electric heater ($350\text{ }^{\circ}\text{C}$ approximately). And, the right side of batteries in the last row was the air environment ($20\text{ }^{\circ}\text{C}$ approximately), which weakened the heat hazard. TR occurred in the batteries of middle row by the higher temperature of batteries in the first row ($> 700\text{ }^{\circ}\text{C}$), which resulted in the batteries in the middle row with the highest temperature. However, the temperature of middle battery was the least when the SOC of battery module was 100%. This is because a lot of heat was depleted during TR occurred inside battery in the middle row due to the ejection of materials. Additionally, T_{max} presents a slightly higher owing to the strong exothermic reaction in higher SOC [66]. For example, the highest temperature of battery #1 with 60% SOC was $754.5 \pm 29.3\text{ }^{\circ}\text{C}$, while T_{max} of battery #1 with 80% SOC and 100% SOC were 766.0 ± 55.9 and $862.7 \pm 60.3\text{ }^{\circ}\text{C}$, respectively. The onset temperature of TR (T_r) of batteries become lower with TR propagation process for various SOC. This is because the T_{max} (such as $754.5 \pm 29.3\text{ }^{\circ}\text{C}$ for 60% SOC) and temperature rise (\dot{T}) (such as $11 \pm 0.1\text{ }^{\circ}\text{C/s}$ for 60% SOC) of first row battery are higher than these of heater ($350\text{ }^{\circ}\text{C}$ and $10\text{ }^{\circ}\text{C/min}$, respectively). The external high heat increased the active materials in battery. Hence, the temperature rising rate of TR (\dot{T}) of batteries become higher

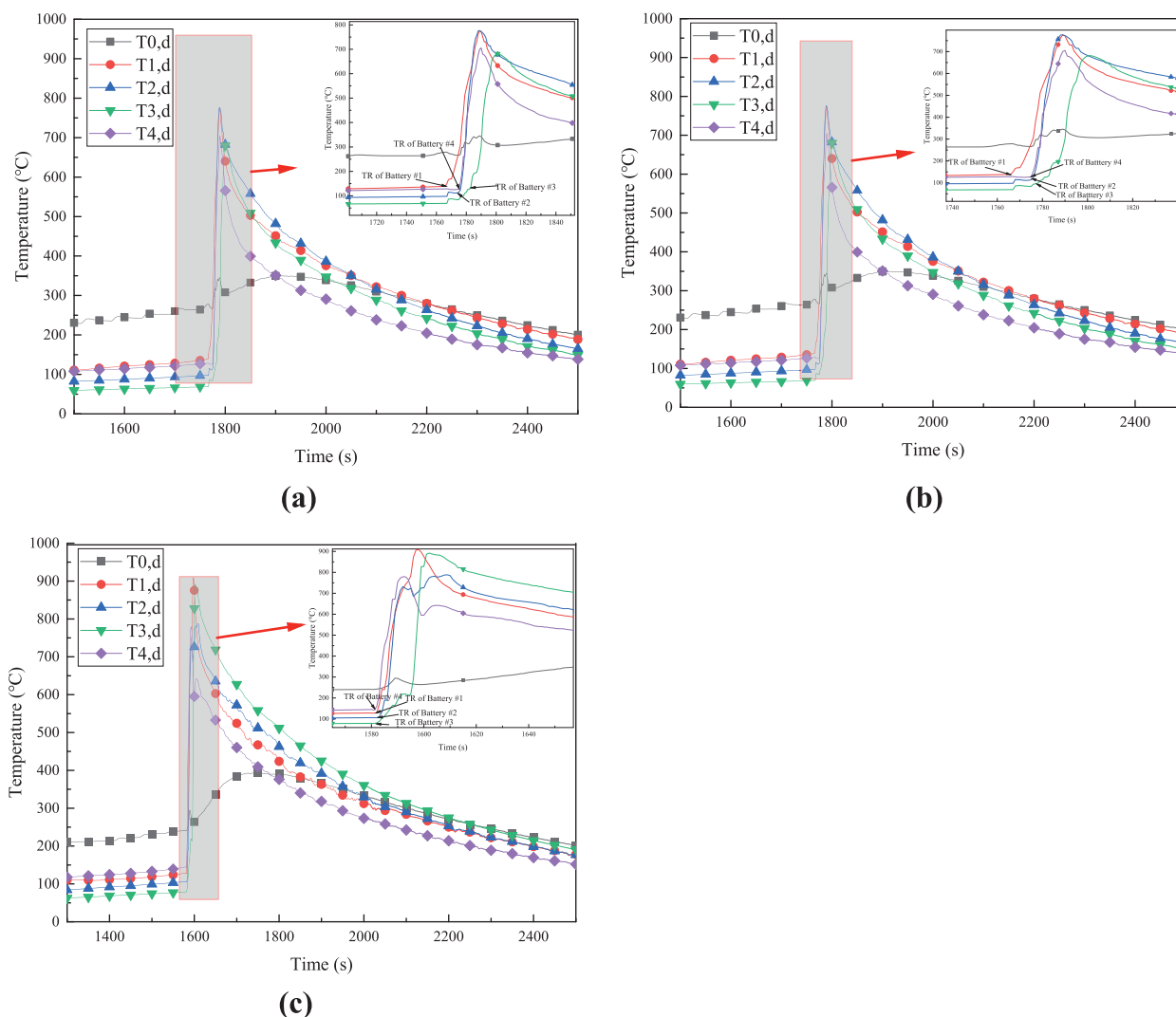


Fig. 6. Surface temperature of battery module of various SOC: (a) 60 %; (b) 80 %; (c) 100 %.

with TR propagation process for 60 % SOC and 80 % SOC. Additionally, \dot{T} increased and T_r decreased in battery module with higher SOC (i.e., 80 and 100 %). This indicated that battery modules with higher SOC bring more heat hazard.

Fig. 7(a) shows the responsive time of battery module with various SOC. The responsive time (t_{re}) of TR become longer from left to right battery in module, which accords with the rule of TR propagation. It took 1992 s to finish the TR propagation process at 60 % SOC. It took 1883 s for the battery module to finish TR propagation at 80 % SOC, and consumed 1865 s at 100 % SOC. TR happened inside batteries became early with the increasing of SOC owing to lower T_r , as shown in Fig. 7(b). Fig. 7(b) presents the variations in the onset temperature of TR when the temperature rate overpass 10 °C/s. The onset temperature of TR in batteries decreased with the increasing of SOC. It is noticeable that T_r of battery #2 with 60 % SOC was unusually low. This maybe because the surface temperature could not completely represent the actual temperature in the battery #2. The different battery with same SOC shows different T_r . This maybe the big temperature gradient between the surrounding cells accelerate the heat transfer, which result in the lower T_r .

Fig. 8 shows the battery temperature rate curves of battery #1 and battery #2 in battery module with 60 % SOC. The battery #1 occurred a quasi-exponential rise process with temperature. Before battery went into TR, the temperature rate was fluctuated because battery self-heating could not ensure the rate of temperature rise increase.

Subsequently, a remarkable amount of heat released during TR occurred inside battery #1, which led to temperature rise quasi-exponential increased with temperature. TR inside battery #1 was started at the temperature rate of 11 °C/s. Concurrently, the high temperature gradient between batteries brought the heat transfer, which resulted in temperature rate of battery #2 rapid enhanced. Hence, TR inside battery #2 was activated at the rate of temperature rise of 34 °C/s. Hence, heat transfer between batteries during TR propagation increases the thermal hazard of battery.

Fig. 9 shows typical TR propagation process of battery module with 60 % SOC. As shown in Fig. 9, the battery module experienced a TR propagation process (#1 → #4 → #2 → #5 → #6 → #3), which is consist with temperature curve (Fig. 6(a)). Firstly, the safety valves of battery #1 and battery #4 opened one after another with a loud crack. The open event of safety valve was accompanied with release of some smoke. Then, the release rate of these combustible smokes continuously accelerated with increasing gradually of battery temperature. Finally, a considerable of smoke produced by battery #1 was ignited by sparks. The TR occurred inside battery #1 only 1 s after the battery was ignited. At the moment, a high-speed jet fire was observed, forming white light zone, which indicated violent chemical exothermic reactions happened inside battery. These chemical exothermic reactions often generate a lot of combustible gases, which result in these gases eject from safety valve with high-speed. Finally, these combustible gases were ignited by the

Table 3
Significant parameters of batteries during TR propagation.

Battery number		#1	#2	#3	#4
60 % SOC	T_{max} (°C)	754.5 ± 29.3	786.1 ± 13.3	702.6 ± 29.3	705.4
	T_r (°C)	152.9 ± 19.2	113.0 ± 1.2	129.6 ± 6.2	127.5
	t_{re} (s)	1977 ± 298	1981 ± 292	1992 ± 295	1775
	\dot{T} (°C/s)	11	22.2 ± 16.7	32.5 ± 14.2	26.1
	T_{max} (°C)	766.0 ± 55.9	763.8 ± 74.7	743.4 ± 87.1	752.9 ± 52.8
80 % SOC	T_r (°C)	152.3 ± 12.1	129.5 ± 32.6	114.4 ± 8.6	153.9 ± 23.5
	t_{re} (s)	1870 ± 103	1872 ± 104	1883 ± 148	1871 ± 100
	\dot{T} (°C/s)	24.3 ± 11.5	30.3 ± 14.2	95.5 ± 118.5	38.3 ± 10.7
	T_{max} (°C)	862.7 ± 60.3	693.5 ± 156.6	895.7 ± 5.1	807.4 ± 30.3
	T_r (°C)	124.0 ± 4.2	110.1 ± 16.2	87.4 ± 1.7	144.3 ± 5.3
100 % SOC	t_{re} (s)	1820 ± 290	1822 ± 290	1865 ± 398	1816 ± 286
	\dot{T} (°C/s)	75.9 ± 87.3	27.6 ± 20.0	13 ± 1.4	23.6 ± 17.2

preceding flame, which was conducive to the forming of jet fire. Generally, TR accompanied with jet fire occurred after it was ignited, which was also observed in previous research [66]. Similarly, the battery #2, battery #4 and battery #3 occurred jet fire and even explosion after these batteries were ignited. Additionally, an interesting phenomenon was observed that the ignition event of other batteries occurred almost simultaneously with the opening of the relief valve except battery #1 and battery #4. This is because battery #1 and battery #4 became the ignition source of subsequent batteries in modules, which accelerated the process of TR of these batteries. The heat conduction and the thermal radiation from TR of battery #1 and battery #4 increased the thermal hazard for the battery #2 and battery #5, and the similar TR phenomenon was observed in battery #3 and battery #6. TR happened in battery #2 prior to that in battery #5 owing to the heat move from battery #1 to battery #2. Finally, TR initiated in battery #6 and battery #3 owing to heat transferring of battery #5 and battery #2, respectively.

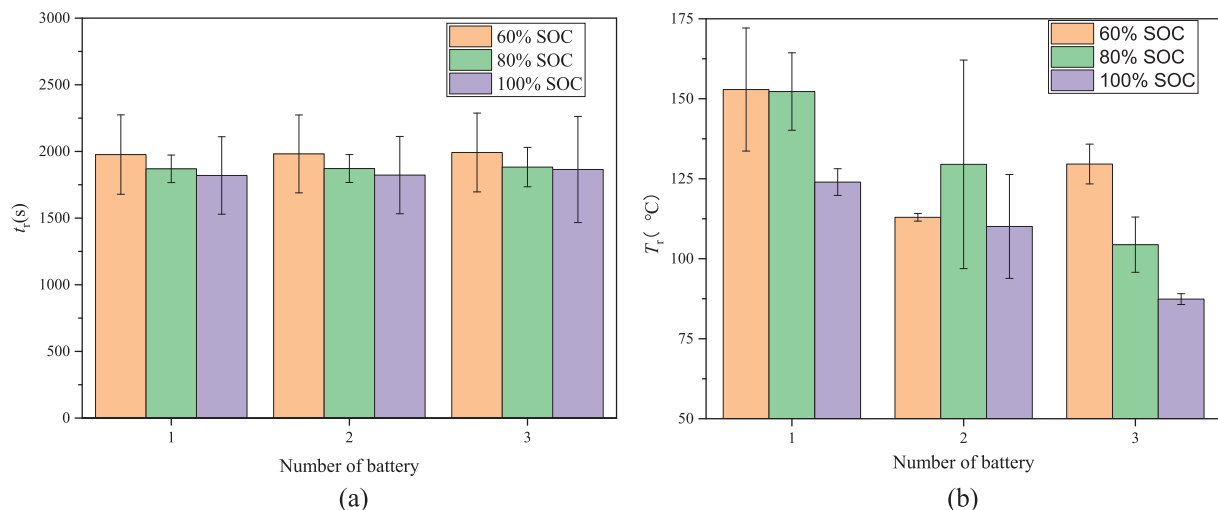


Fig. 7. (a) Responsive time (t_{re}) of TR with various SOC; (b) onset temperature of TR (T_r) with various SOC.

3.2. Suppressing effect of WM on TR propagation

To understand the cooling and extinguishing effect of pure water, WM was investigated for different SOC module. The variations in the surface temperatures of the batteries experienced for battery module with different SOC were illustrated in Fig. 10. The light blue rectangle represents the duration of WM release, including moment of application and duration time. In this work, the moment of WM release was on fire of the first battery and the duration time of WM was 30 s in all the tests. In the test 4, when the first battery (battery #1) caught fire, the WM was applied. The batteries in battery module with 60 % SOC not experienced TR at the moment, while the surface temperature of battery #1 was 192.3 °C. Although the temperature was lower than the onset temperature of TR inside battery #1 (197.1 °C), WM could not efficiently suppress the TR inside battery #1 in the following time. WM needed some time to completely penetrated into the battery module due to the existing of flame. Additionally, the cooling of battery mainly relies on the vaporization latent heat and specific heat of water, thus the theoretical cooling power of battery dissipated can be expressed using:

$$P_w = \begin{cases} c_w m_w (T - T_0); & T < T_{boil} \\ c_w m_w (T_{boil} - T_0) + h_f m_w; & T \geq T_{boil} \end{cases} \quad (2)$$

where C_w represents the specific heat (4.12 kJ/kg•°C); h_f is the vaporization latent heat of water (2257 kJ/kg) and m_w is the mass of water laid on the battery surface. T is the battery temperature (°C), T_0 is the environment temperature (20 °C) and T_{boil} is the boil temperature of water (100 °C). The m_w can be figured out as follows:

$$m_w = \rho_w \dot{q}_w \quad (3)$$

where ρ_w is the density of water (1000 kg/m³) and \dot{q}_w represents the volume flow rate of WM on a single cell (8.0×10^{-8} m³/s). Thus, the cooling power is 206.93 W. The heating power of battery can be calculated using: [66].

$$P_H = m_b c_b \dot{T} \quad (4)$$

where m_b is the mass of cell after test, \dot{T} is the battery temperature (°C) and c_b is the specific heat of battery (1.1 kJ/kg•°C). Fig. 11 shows the P_H curve of the first battery occurred fire in the test 1. The P_H was 458.3 W when TR occurred in the battery and reached the maximum value of 2084.5 W. Therefore, WM could not suppress the TR in battery #1 because cooling power is far less than heating power. As illustrated in Fig. 10(a), T_{1max} reached a maximum temperature of 739.3 °C during the WM application. Subsequently, the P_H rapidly reduced -88.4 W in

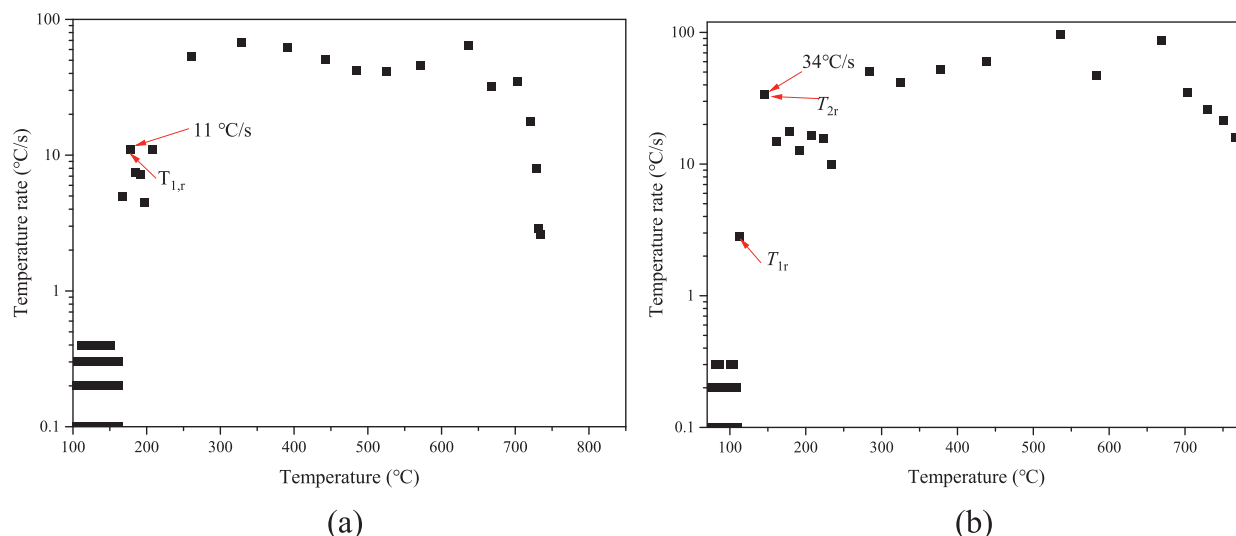


Fig. 8. Temperature rate curve of battery module with 60 % SOC: (a) battery #1; (b) battery #2. $T_{1,r}$ is the point corresponding to the thermal runaway of battery #1. $T_{2,r}$ is the point corresponding to the thermal runaway of battery #2.

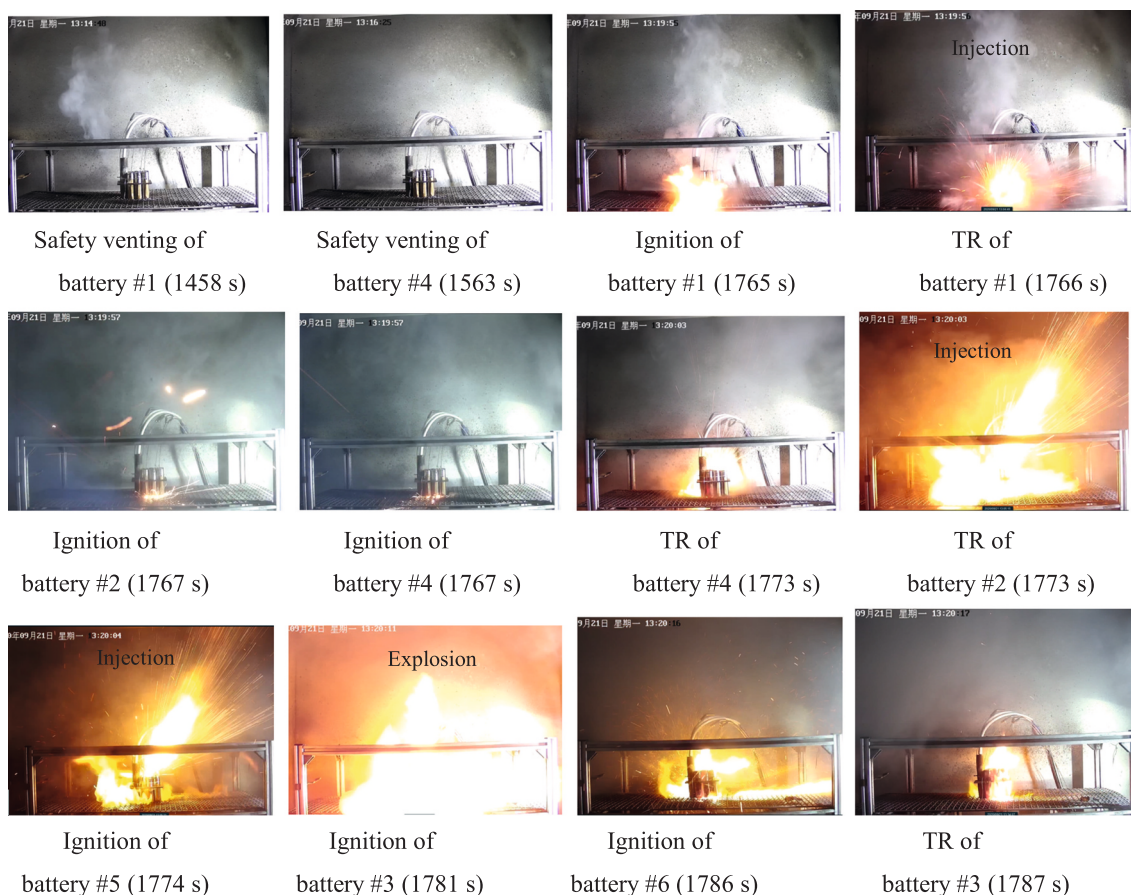


Fig. 9. TR propagation process of 60 % SOC battery module.

19 s due to momentary heating process. Finally, the temperature of battery #1 reduced due to the cooling power of WM dominated the temperature variation. However, battery #4 and battery 2 went into TR during the WM release. The $T_{4,max}$ reached a maximum of 300 °C approximately during the WM application. The heat power of battery #2 was related to heat transfer with battery #1 and battery self-heating. Hence, the surface temperature of battery #2 rebounded during the

WM application. The fire was extinguished 26 s after WM was released. The battery #3 was successfully controlled during WM was applied. The surface temperature of battery #3 increased slightly at early stage of WM release and rapidly reduced from 143.7 °C to 66.3 °C in 10 s due to water cooling. Then, a liquid film warped the surface of battery #3 and cooling capacity of water become worse due to below 100 °C, as shown in Eq. (2). Hence, the temperature of battery #3 slightly increased to

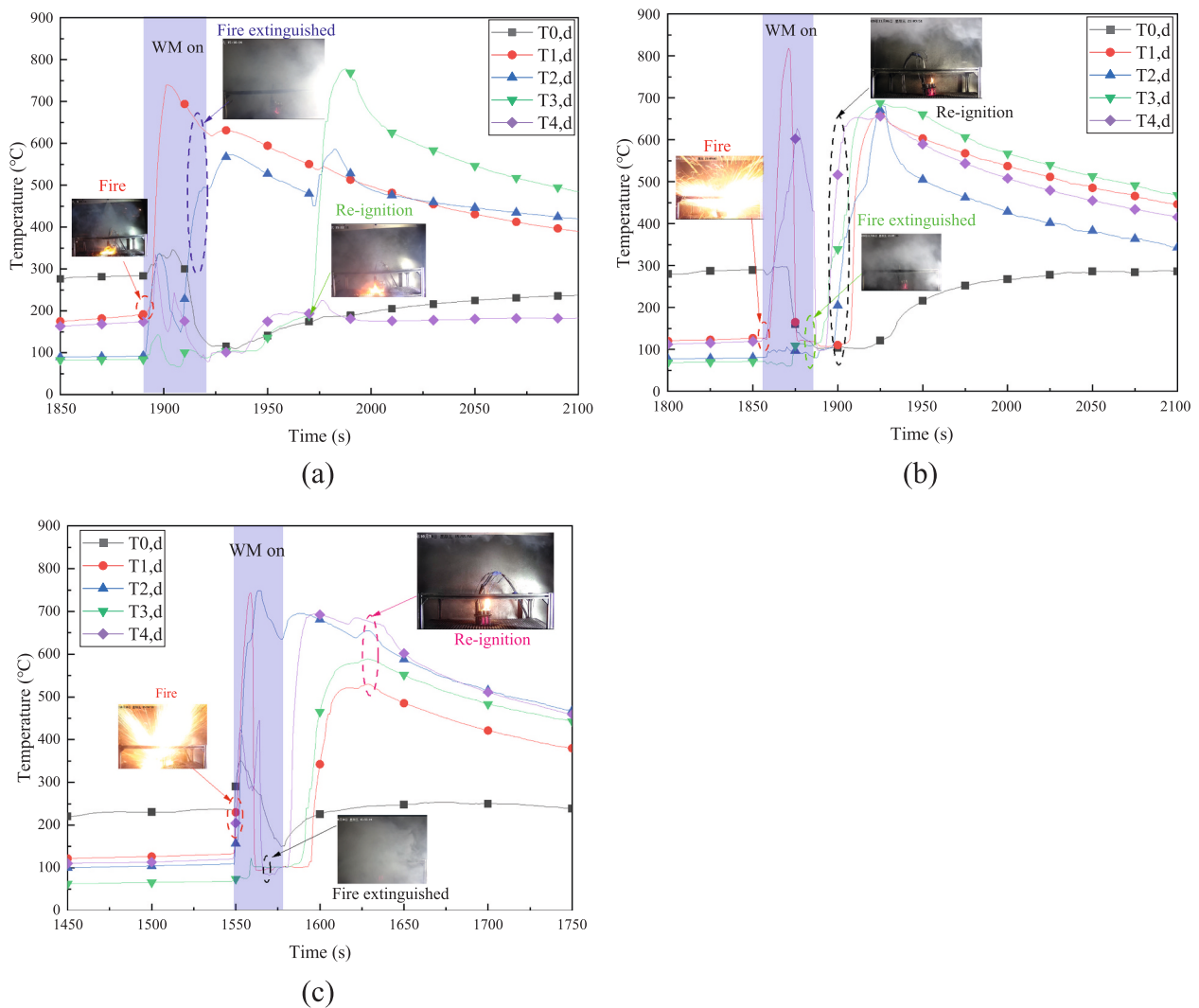


Fig. 10. Surface temperature of battery module during WM application: (a) 60 % SOC; (b) 80 % SOC; (c) 100 % SOC.

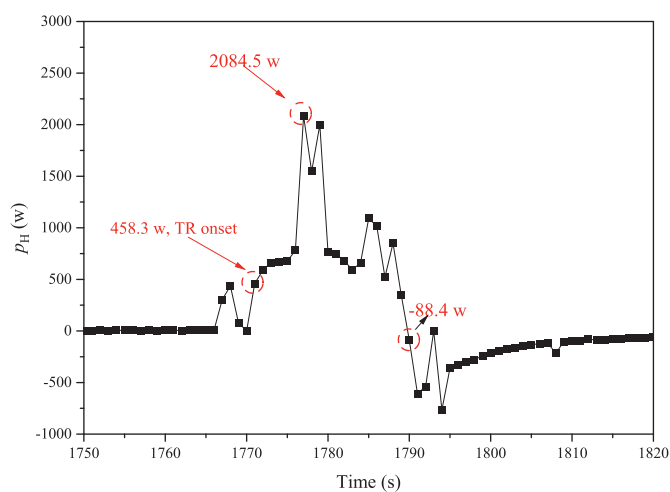


Fig. 11. Change curves of heating power (p_H) inside battery #1 in test 1.

106.3 °C owing to heat transfer of battery #2 and the liquid film dried up. Then, the surface temperature of battery #3 decreased to 87.8 °C at late stage of WM application. Hence, a new liquid film was formed on

the surface of battery #3. All the cells in the module indicated a slight increase due to the residual heat inside the cells after WM applied. Finally, the battery #3 occurred fire and TR in the condition of heat transfer of battery #2. The maximum surface temperature of battery #3 reached 777.7 °C.

The battery module with 80 % SOC and with 100 % SOC experienced a similar temperature curves, as shown in Fig. 10(b-c). It took approximately 30 s to extinguish open fire of 80 % SOC battery module by WM, while consumed 24 s to suppress the open fire of 100 % SOC module. This is because rapid combustion of 100 % SOC module accelerates the extinguishment process. Although the open fire of these higher battery modules (80 % and 100 % SOC) was extinguished during the WM was released, all the batteries happened jet fire and TR. Table 4 presents the significant parameters of batteries in test 4-6. The maximum temperature of batteries increased with increase of SOC. This indicated that the difficulty of suppressing TR propagation become bigger with increasing of SOC. The surface temperatures of all the batteries rapidly rebounded higher after the WM application. This phenomenon maybe contribute to the fact that the internal temperature of battery was still high and without significantly reduced during the application of WM [70]. The internal heat of battery transferred to the battery surface though battery shell. Additionally, the open fire of 80 % SOC module was observed again in the process of temperature rise, while the open fire of 100 % SOC module was observed after the peak temperature. This maybe the

Table 4
Key parameters of battery module during WM with different SOC.

Battery number		#1	#2	#3	#4	
60 % SOC	T_{max} (°C)	635.1 ± 147.9	586.2 ± 18.5	762.3 ± 21.8	335.9	
	T_r (°C)	171.7 ± 35.9	94.8 ± 3.4	91 ± 5.8	178.7	
	t_{re} (s)	1787 ± 148	1789 ± 144	1791 ± 143	1892	
	\dot{T} (°C/s)	10.7 ± 0.6	33.5 ± 13.3	30.4 ± 6.0	25.5	
	T_R (°C)	591.2 ± 69.7	579.9 ± 9.6	425.6 ± 454	101	
	80 % SOC	T_{max} (°C)	808.0 ± 14.6	633.8 ± 65.5	627.5 ± 85.6	617.0 ± 55.6
		T_r (°C)	146.8 ± 4.0	108.3 ± 0.5	111.6 ± 8.3	112.4 ± 22.8
t_{re} (s)		1847 ± 19	1869 ± 40	1871 ± 28	1848 ± 14	
\dot{T} (°C/s)		61.3 ± 15.3	19.4 ± 10.8	31.6 ± 19.8	25.5 ± 7.6	
T_R (°C)		665.2 ± 9.5	619.4 ± 89.7	627.5 ± 85.6	617.0 ± 55.6	
100 % SOC		T_{max} (°C)	913 ± 239.0	799.2 ± 71.0	668 ± 112.8	681.4 ± 18.2
		T_r (°C)	139.0 ± 5.3	109.0 ± 0.9	85.0 ± 6.0	112.5 ± 22.8
	t_{re} (s)	1724 ± 247	1724 ± 248	1734 ± 249	1725 ± 249	
	\dot{T} (°C/s)	63.1 ± 45.1	62.2 ± 18.6	32.1 ± 14.6	46.1 ± 42.5	
	T_R (°C)	635 ± 148.6	701 ± 8.2	623 ± 50.0	681.3 ± 18.4	

higher SOC (100 % SOC) has been consumed during the WM application. Different with TR of battery #3 in the 60 % SOC module, the re-ignition of these high SOC modules happened on the whole the module. Clearly, WM has poor effect to fight with the re-ignition. Therefore, to improve the cooling efficiency and extinguishment, a kind of micelle encapsulator was investigated for the battery module fire.

3.3. Suppressing effect of a micelle encapsulator on TR propagation

Fig. 12 presents the effective suppression of 3 % F-500 solution on battery module fire in test 7–9. The sight orange rectangle is the duration of F-500 release. The same as the release time of WM, 3 % F-500 solution was released when the first battery in battery module occurred fire. However, TR inside the battery #1 and battery #4 occurred during the 3 % F-500 solution application. The surface temperature of battery #1 reached 276.4 °C at early stage of application, then the temperature was rapidly decreased. Fortunately, other batteries were protected due to their retaining low temperature, as shown in Fig. 12(a). It took 15 s to completely put out the flame in test 7. The surface temperatures of battery #1 and battery #4 rebounded after the application due to internal heat of batteries transferring. As shown in Table 5, The rebounded temperatures of battery #1 and battery #4 were 286.7 °C and 319.8 °C, respectively. In addition, the temperatures of other batteries were not obviously rebounded. Same conclusion as WM, the difficult of fighting fire became bigger with increasing of SOC for 3 % F-500 solution. It consumed 19 s to suppress the battery module with 80 % SOC fire for 3 % F-500 solution. The maximum surface temperature of battery #1 was 748.4 °C during 3 % F-500 solution application. Then, the temperature was rapidly reduced. The TR happened in the battery #1, battery #4 and battery #2 with 80 % SOC battery module during 3 % F-500 solution application. Although the surface temperature of battery #1, battery #4 and battery #2 happened rebound after 3 % F-500 solution application, no open fire was observed. Therefore, rapid extinguishing flame was positive to cool the battery module. All the temperatures of batteries rebounded after 3 % F-500 solution application. As illustrated in Table 5,

the rebounded temperatures of battery #1, battery #4 and battery #2 were 385.5, 382.9 and 419.3 °C, respectively. It is indicated that 3 % F-500 solution could not suppress TR propagation of battery module with 100 % SOC. Apparently, the rebounded temperature of batteries with higher SOC became bigger. Fortunately, no open fire was observed for battery module with 100 % SOC after 3 % F-500 solution application. In addition, the onset temperature rise became bigger with increasing of SOC, as shown in Table 5. The difficult of fighting fire became bigger with increasing of SOC for 3 % F-500 solution. In a word, compared with WM, 3 % F-500 solution showed excellent suppressing flame capacity and outstanding resistance ability to re-ignition.

3.4. Extinguishment mechanisms of micelle encapsulator

3.4.1. Gas analysis under various SOC

In the blank experiment of gas analysis, most of gas are helium, so it is considered that the tightness of the device is good. In the subsequent experimental results, helium will be detected and ignored in order to express intuitively. Fig. 13 shows the main gas ingredients of tested battery with different SOC. The detected gas ingredients were H₂, CO, C₂H₄, CH₄ and CO₂, which were consistent with the previous empirical studies [85,86]. Obviously, these released gases were flammable and explosive. H₂ and CO were key flammable components, so they were chosen characterized gases of battery in following work. The proportions of CO and H₂ in TR gases of battery with 60 % SOC were 34.95 % and 16.31 %, respectively. Compared battery with 60 % SOC, the battery with 80 % SOC possessed higher the proportion of H₂ in TR gases, which reached 23.3 %, while the proportion of CO reduced to 27.6 %. The proportion of CO was the highest when SOC of battery increased 100 %, which reached 40.17 %. The proportion of H₂ was 20.73 % when the battery with 100 % SOC. Additionally, the proportion of CO₂ almost decreased with increase of SOC. The proportion of CO₂ was 40.78 % when the battery possessed 60 % SOC, and proportion of CO₂ for battery with 80 % and 100 % were 41.4 % and 32.05 %, respectively. Other gases, such as C₂H₄ and CH₄, have no obviously difference with different SOC.

3.4.2. Gas absorption mechanism analysis of 3 % F-500 solution

As shown in Fig. 14, the different fire-extinguishing agents were found to play a significant role in the extinguishment effectiveness of the battery module. Combustion time without any fire-extinguishing agents was longer than the time under the condition of WM. The combustion time of battery module become short with the increasing of SOC due to violent chemical reaction inside battery at high SOC. The combustion time of battery module with 60 %, 80 %, 100 % SOC were 54 ± 9, 42 ± 11 and 41 ± 1 s, respectively. The result indicted that WM was positive to fight the fire. The SOC have almost no effect on the extinguishment efficiency of WM. It took appropriately 25 s for WM to battery module. However, open fire was observed after the fire was extinguished in test 4–6. 3 % F-500 solution consumed 18 ± 4, 17 ± 8 and 29 ± 1 s, respectively to extinguish battery module fire with 60 %, 80 %, 100 % SOC, as shown in Fig. 14. Fortunately, re-ignition phenomenon was not observed when 3 % F-500 solution was applied, as discussed in Section 3.3. Clearly, compared with pure WM, the 3 % F-500 solution possessed excellent extinguishing effective. The Fig. 15 shows the extinguishment mechanisms of WM and 3 % F-500 solution, respectively. The extinguishment mechanisms of WM mainly depend on the cooling, suffocation and insulation [87]. When WM released, it diluted the oxygen in the air above the battery by suffocation, as shown in Fig. 15(b). Meanwhile, the concentrations of combustible gases were reduced by the isolation. The flame zone above the battery module was cooled due to the steam conversion of WM. However, WM was not effective (>20 s) by rapidly suppressing the flame. This is because liquid droplets of WM with low thermal mass cannot reach the heat source of battery module [88].

By contrast, the efficiency of 3 % F-500 solution on extinguishing battery module flame was better than WM. A very important feature of

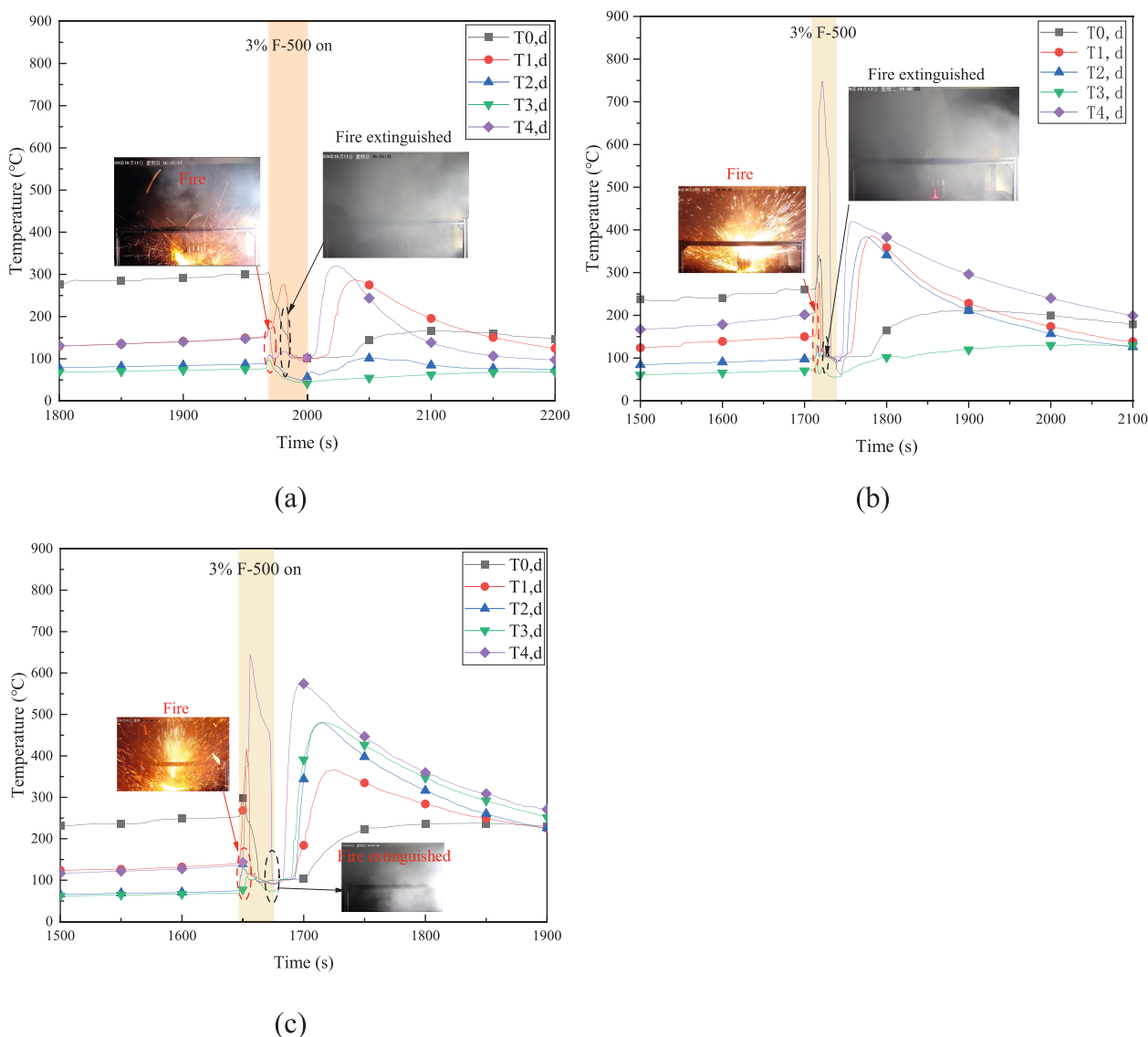


Fig. 12. Temperature variation for surface of test 7-9 extinguished by 3 % F-500 solution: (a) 60 %; (b) 80 %; (c) 100 %.

LIBs fire compared with ordinary fire is that LIBs fire will produce a large number of combustible gases, such as CO and H₂, which are difficult to dissolve in water, so WM is difficult to deal with these gases. 3 % F-500 could put out open flame by encapsulating the combustible gases. The main composition of F-500 is a kind of amphiphilic surfactant, whose polar head could dissolve in water, and the nonpolar tail repel water molecules seeking other types of molecules, such as hydrocarbons [89]. As shown in Fig. 15(c), A group of F-500 molecules can arrange around the hydrocarbon molecules to form a microcellular called “Chemical Cocooning”, which causes the hydrocarbon molecules to lose their flammability. The wrapped combustible gases flowed away with the agent. For SOC100 % LIBs, WM and 3 % F-500 cannot completely extinguish the battery fire, but the effect of F-500 on WM is better, which slows down the combustion rate of the battery.

Fig. 16 shows the micelle size of 3 % F-500 solution after absorption tests. We found that the micelle size of 3 % F-500 solution became bigger after absorption tests than before, which indicated that 3 % F-500 solution could absorb these key gases. The median particle diameter (D50) of 3 % F-500 solution was 38.15 nm before absorption tests. The D50 of 3 % F-500 solution after the absorbed H₂ was 49.76 nm, and the D50 of 3 % F-500 solution after absorbed CO was 81.73 nm. This is because the main elements of F-500 is an amphiphilic surfactant, which

contains a hydrophilic group and a lipophilic group [90]. The lipophilic group caught CO and H₂ in the micelle, which resulted in variation of the volume and the cumulative distribution of the micelle. The F-500 has a polar head end and a non-polar tail end. H₂ is a non-polar gas and CO is a weakly polar molecule. Therefore, H₂ and CO are easily captured by the non-polar side of F-500, and H₂ and CO will be wrapped in the micelle. The Gibbs free energy decreases in this process, so the gas absorption is a spontaneous process. Based on Mukerjee model [91], the chemical potential energy of gases molecule increases caused by Laplacian force in the micelle, which contributes to gas molecule entering the micelle. The increment of free energy (ΔG) can be the Eq. (5) as follows:

$$\Delta G = \Delta P_L \bar{V}_m = \frac{2\gamma \bar{V}_m}{r} \quad (5)$$

where ΔP_L is the Laplacian force from the interface of micelle and water; and γ is the interface force between micelle and water. $1/r$ is the curvature of micelle and \bar{V}_m is partial molar volume of gas. Hence, the combustible gases were isolated from oxygen by water layer. In addition, the heat from the combustible gases was conveyed from the inner to outer, as shown in Fig. 15(c). It was also found that the micelle size of 3 % F-500 solution after absorbed CO increased slightly bigger than absorbed H₂, because molecule size of CO is the bigger than H₂.

Table 5
Key parameters of battery module during 3 % F-500 solution with different SOC.

Battery number		#1	#2	#3	#4
60 % SOC	T_{\max} (°C)	216 ± 100.0	105.9 ± 4.2	85.9 ± 15.5	359.4 ± 55.9
	T_r (°C)	177.4	–	–	165.2 ± 12.7
	t_{re} (s)	1972	–	–	1840 ± 182
	\dot{T} (°C/s)	12.3	–	–	17.9 ± 11.2
	T_R (°C)	192.2 ± 133	69.5 ± 0.5	63.8 ± 14.3	296.3 ± 33.3
	T_{\max} (°C)	385.5	382.9	130.1	748.4
80 % SOC	T_r (°C)	156.1	107	–	205.9
	t_{re} (s)	1715	1714	–	1714
	\dot{T} (°C/s)	16.2	24.1	–	80
	T_R (°C)	385.5	382.9	103.3	419.3
	T_{\max} (°C)	478.7 ± 86.4	467.9 ± 17.5	610 ± 184.9	682.5 ± 54.5
	T_r (°C)	114.2 ± 41	65.2 ± 13.5	125.9 ± 78.6	148.6 ± 6.8
100 % SOC	t_{re} (s)	1767 ± 169	1772 ± 177	1869 ± 308	1766 ± 165
	\dot{T} (°C/s)	16.2 ± 0.8	30.5 ± 8.5	24.1 ± 4.7	33.0 ± 26.5
	T_R (°C)	452.7 ± 123.2	467.9 ± 17.5	610.7 ± 184.9	653.3 ± 110.7

3.4.3. Cooling mechanism analysis of 3 % F-500 solution

An assessment of rebounding temperature is significant in evaluation of cooling capacity and resistance ability to re-ignition. Fig. 17 shows the temperature curve of the first battery with different SOC. The surface temperature of battery was rapidly reduced to below 100 °C, then the temperature rapidly reached to a relative low temperature, as shown in Fig. 17. The second peak temperature value was defined as the rebounding temperature in this work. Fig. 18(a) shows the rebounding temperature of first battery when WM was applied. The impact of WM on the rebounding temperature was not obviously, which indicated that the cooling capacity of WM was poor. The rebounding temperature of first battery was 664.1 ± 11.0 °C in the test 5. Obviously, the rebounding temperature was enough to cause TR propagation of all battery, as shown in Fig. 18(b). The rebounding temperature lower the $414.8.5 \pm 6.4$ °C was enough to prevent thermal runaway propagation. In addition, the rebounding temperatures of first battery increased with the increasing.

of SOC when 3 % F-500 solution was discharged, as shown in Fig. 18 (a). The rebounding temperatures when 3 % F-500 solution was released were less than that when WM was released. This is because 3 % F-500 solution possesses higher cooling capacity than WM. Fig. 19 shows the viscosity and surface tension of 3 % F-500 solution and pure water. The

viscosity and surface tension of 3 % F-500 solution were 2.05 Mpa•s and 23 MN/m, respectively. However, the viscosity and surface tension of pure water were 1.1 Mpa•s and 69 MN/m. Compared with pure water, 3 % F-500 solution possessed lower surface tension. The lower surface tension reduced the droplet size of water, which increased the contact surface with fire zone. Additionally, the lower surface tension increased the contact surface with battery module, which improved the penetration performance of water. The outstanding penetration capability allowed more water to rapidly contact the battery module and attack hidden fires of battery module successfully when 3 % F-500 solution was applied. Therefore, 3 % F-500 solution could absorb more heat than pure water. Additionally, cooling capacity is also positive to prevent the re-ignition of battery module. Re-ignition also need three conditions, as discussed in Section 1. Almost fire-extinguishing agents could not reach to the inner of battery owing to its special construction. It is difficulty to remove the fuel and oxygen after the fire-extinguishing agent was released. Meanwhile, oxygen is also provided by battery. Therefore, cooling effect dominated the re-ignition. This is reason why no re-ignition was observed after 3 % F-500 was applied, as discussed in Section 3.3.

4. Conclusions

We studied the gases released from the battery by experiments and the extinguishment mechanisms of 3 % F-500 solution. The following

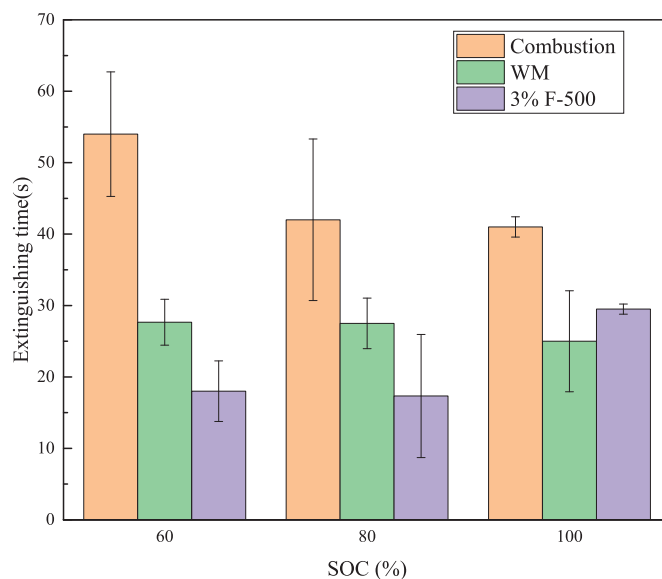


Fig. 14. Extinguishing time of different fire-extinguishing agents of different SOC.

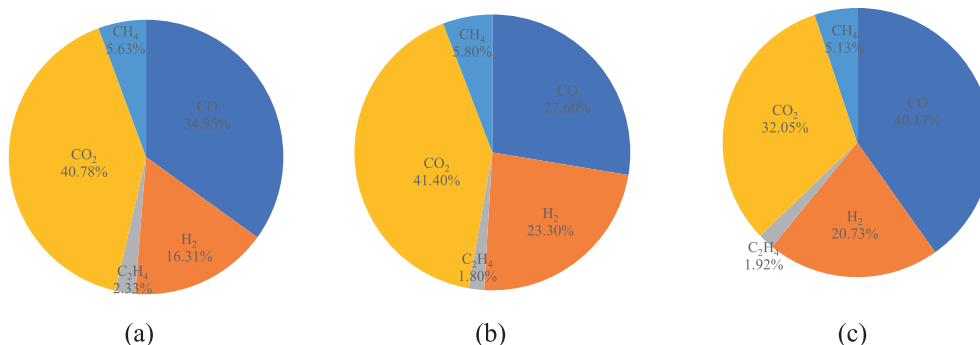


Fig. 13. Detected components of the released gases (vol%): (a) 60 %; (b) 80 %; (c) 100 %.

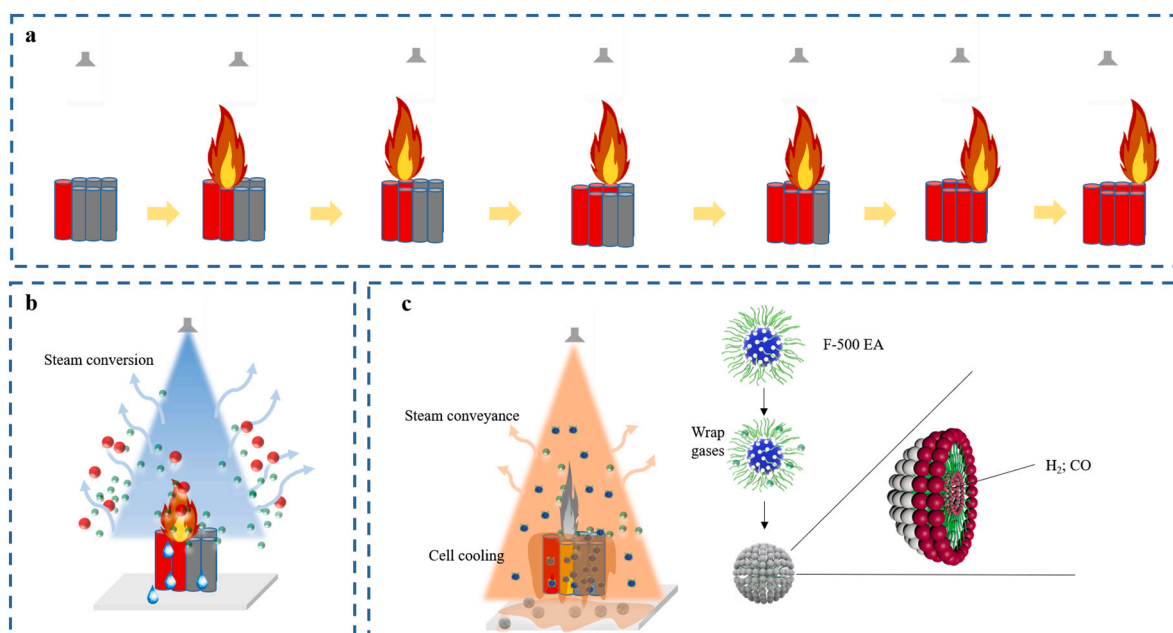


Fig. 15. Extinguishment mechanisms of fire extinguishing agents: (a) TR propagation phenomenon in the test; (b) extinguishment mechanisms of WM, the red balls is oxygen molecules, the green balls are hydrocarbon combustible molecules (c) extinguishment mechanisms of F-500. (For interpretation of the references to colour in this figure legend, the reader is referred to the web version of this article.)

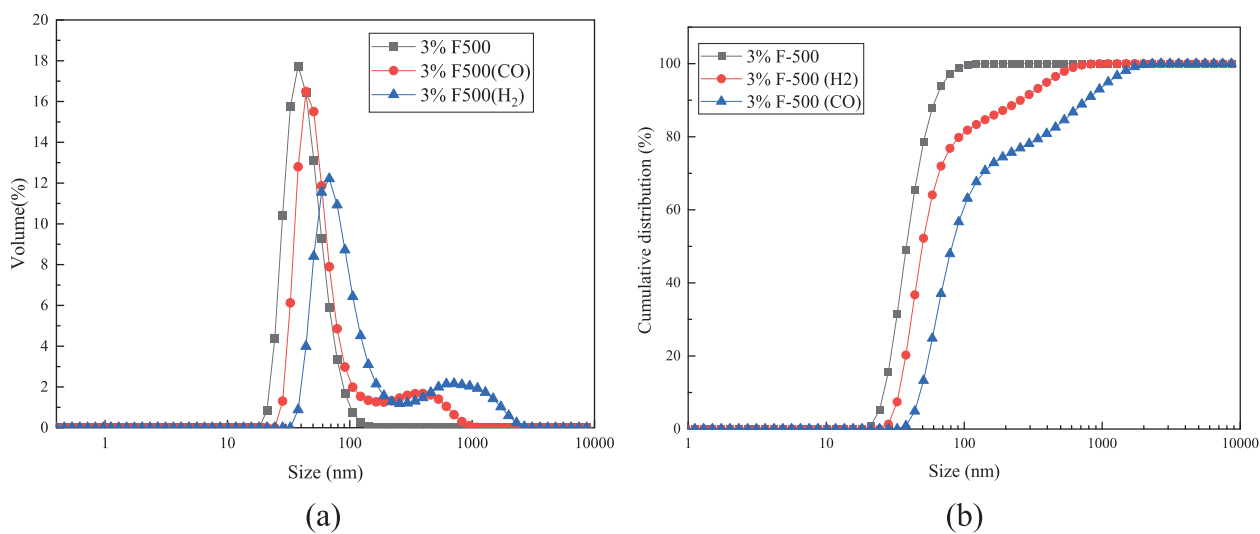


Fig. 16. Micelle size of 3 % F-500 solution before and after absorption tests: (a) volume distribution curve of micelle size; (b) cumulative distribution curve of micelle size.

points could be found from this work:

- (a) The gases released from battery were combustible and explosive. Hydrogen and carbon monoxide account for the largest proportion of combustible components released from TR occurred in the battery.
- (b) It was proved that 3 % F-500 solution could absorb the key explosive gases. The micellar size of 3 % F-500 solution after absorbed test was bigger than before (D50 from 38.15 nm to 49.76 nm for H₂ and 81.73 nm for CO, respectively), which indicated that 3 % F-500 solution wrapped the key gases by its micelle structure. Laplacian force in the micelle would be main force to absorb these key gases.
- (c) It was verified that 3 % F-500 solution possessed excellent cooling capacity than WM. 3 % F-500 solution with lower surface tension

and suitable viscosity helped more water to penetrate into battery module. Additionally, cooling mechanism of 3 % F-500 solution on the battery fire depended on transferring heat of fuel. However, the cooling mechanism of WM on the battery module fire mainly relied on heat steam.

- (d) In the test of battery with 60 %, 80 % and 100 %, it is obviously obtained battery module with higher SOC shows less combustion time. However, battery module with higher SOC increased fire-fighting difficulty. More batteries were protected when 3 % F-500 solution was applied than WM in this work.
- (e) At present, there is no perfect solution for the research of LIB fire extinguishing. Through the paper on the fire extinguishing effect and fire extinguishing mechanism of F-500, it is concluded that f-500 has excellent cooling capacity and the ability to absorb the key explosive gases, which can make certain guiding significance

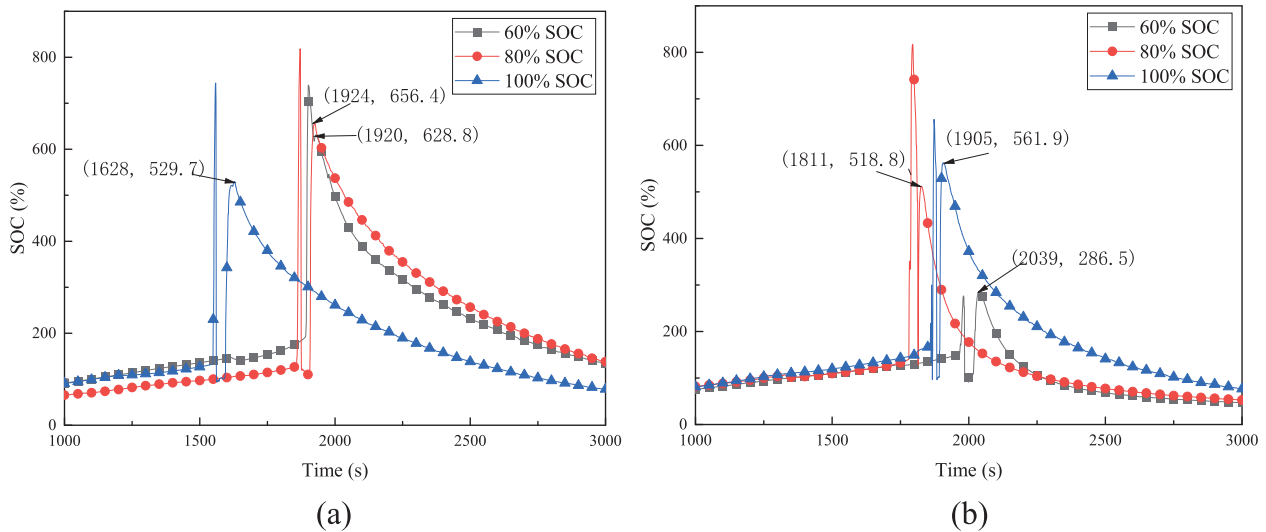


Fig. 17. The temperature curve of first battery: (a) test 4–6; (b) test 7–9.

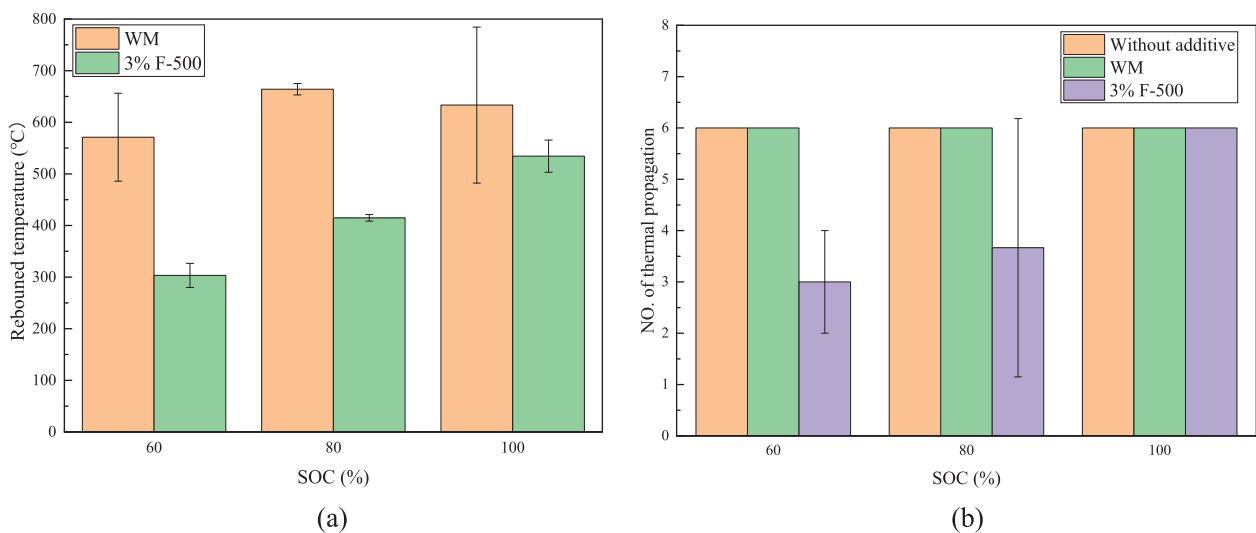


Fig. 18. (a) Rebounding temperature of first battery with different SOC; (b) NO. of TR propagation.

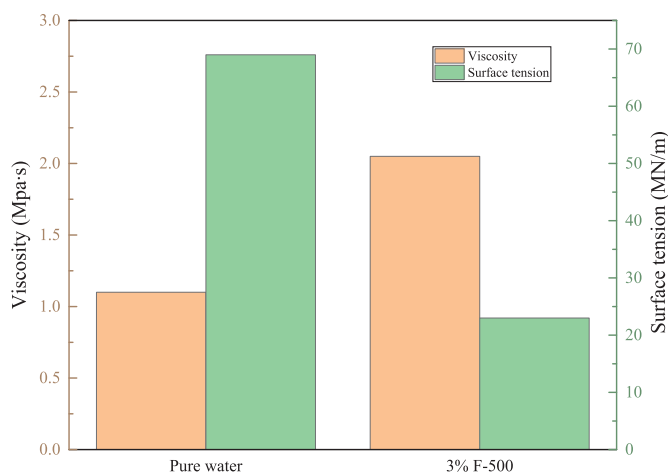


Fig. 19. Viscosity and surface tension results of pure water and 3 % F-500 solution.

for practical application and future research on fire extinguishing agent.

CRedit authorship contribution statement

Shuai Yuan: Conceptualization, Investigation, Validation, Formal analysis, Writing-original draft; Chongye Chang: Conceptualization, Investigation, Validation, Formal analysis, Writing-Review & Editing; Yang Zhou: Methodology, Data Curation; Ruoheng Zhang: Investigation; Jianqi Zhang: Investigation; Yifan Liu: Investigation; Xinming Qian: Conceptualization, Methodology, Project administration, Supervision.

Declaration of competing interest

All authors have read and approved this version of the article, and enough care has been taken to ensure the integrity of the work. No part of this paper has been published or submitted elsewhere. No conflict of interest exists in the submission of this manuscript. I hope you will give favorable consideration to our manuscript and find the article acceptable for publication in your journal. Please contact me if I can be of further assistance. Thank you very much for your attention and

consideration. I am looking forward to hearing from you.

Acknowledgments

This work was supported by the National Key Research and Development Program of China [grant number 2017YFC0804700].

References

- [1] F. Larsson, P. Andersson, P. Blomqvist, A. Lorén, B.E. Mellander, Characteristics of lithium-ion batteries during fire tests, *J. Power Sources* 271 (2014) 414–420, <https://doi.org/10.1016/j.jpowsour.2014.08.027>.
- [2] K. Cavanagh, J. Ward, S. Behrens, A. Bhatt, E. Ratnam, E. Oliver, J. Hayward, *Electrical Energy Storage: Technology Overview and Applications*, Canberra, Australia, 2015.
- [3] X. Feng, J. Sun, M. Ouyang, F. Wang, X. He, L. Lu, H. Peng, Characterization of penetration induced thermal runaway propagation process within a large format lithium ion battery module, *J. Power Sources* 275 (2015) 261–273, <https://doi.org/10.1016/j.jpowsour.2014.11.017>.
- [4] S. Wilke, B. Schweitzer, S. Khateeb, S. Al-Hallaj, Preventing thermal runaway propagation in lithium ion battery packs using a phase change composite material: an experimental study, *J. Power Sources* 340 (2017) 51–59, <https://doi.org/10.1016/j.jpowsour.2016.11.018>.
- [5] C. Tao, Q. Ye, C. Wang, Y. Qian, C. Wang, T. Zhou, Z. Tang, An experimental investigation on the burning behaviors of lithium ion batteries after different immersion times, *J. Clean. Prod.* 242 (2020), 118539, <https://doi.org/10.1016/j.jclepro.2019.118539>.
- [6] X. Feng, S. Zheng, D. Ren, X. He, L. Wang, H. Cui, X. Liu, C. Jin, F. Zhang, C. Xu, H. Hsu, S. Gao, T. Chen, Y. Li, T. Wang, H. Wang, M. Li, M. Ouyang, Investigating the thermal runaway mechanisms of lithium-ion batteries based on thermal analysis database, *Appl. Energy* 246 (2019) 53–64, <https://doi.org/10.1016/j.apenergy.2019.04.009>.
- [7] H. Li, H. Chen, G. Zhong, Y. Wang, Q. Wang, Experimental study on thermal runaway risk of 18650 lithium ion battery under side-heating condition, *J. Loss Prev. Process Ind.* 61 (2019) 122–129, <https://doi.org/10.1016/j.jlp.2019.06.012>.
- [8] Z. Wang, H. Yang, Y. Li, G. Wang, J. Wang, Thermal runaway and fire behaviors of large-scale lithium ion batteries with different heating methods, *J. Hazard. Mater.* 379 (2019), 120730, <https://doi.org/10.1016/j.jhazmat.2019.06.007>.
- [9] F. Larsson, B.E. Mellander, Abuse by external heating, overcharge and short circuiting of commercial lithium-ion battery cells, *J. Electrochem. Soc.* 161 (2014) 1611–1617, <https://doi.org/10.1149/2.0311410jes>.
- [10] L. Huang, Z. Zhang, Z. Wang, L. Zhang, X. Zhu, D.D. Dorrell, Thermal runaway behavior during overcharge for large-format Lithium-ion batteries with different packaging patterns, *J. Energy Storage* 25 (2019), 100811, <https://doi.org/10.1016/j.est.2019.100811>.
- [11] K. Liu, W. Liu, Y. Qiu, B. Kong, Y. Sun, Z. Chen, D. Zhuo, D. Lin, Y. Cui, Electrospun core-shell microfiber separator with thermal-triggered flame-retardant properties for lithium-ion batteries, *Sci. Adv.* 3 (2017) 1–9, <https://doi.org/10.1126/sciadv.1601978>.
- [12] H.F. Xiang, H.Y. Xu, Z.Z. Wang, C.H. Chen, Dimethyl methylphosphonate (DMMP) as an efficient flame retardant additive for the lithium-ion battery electrolytes, *J. Power Sources* 173 (2007) 562–564, <https://doi.org/10.1016/j.jpowsour.2007.05.001>.
- [13] Z. Zeng, X. Jiang, B. Wu, L. Xiao, X. Ai, H. Yang, Y. Cao, Bis(2,2,2-trifluoroethyl) methylphosphonate: a novel flame-retardant additive for safe Lithium-ion battery, *Electrochim. Acta* 129 (2014) 300–304, <https://doi.org/10.1016/j.electacta.2014.02.062>.
- [14] M.F. Rectenwald, J.R. Gaffen, A.L. Rheingold, A.B. Morgan, J.D. Protasiewicz, Phosphoryl-rich flame-retardant ions (FRIONs): towards safer lithium-ion batteries, *Angew. Chem. Int. Ed.* 53 (2014) 4173–4176, <https://doi.org/10.1002/anie.201310867>.
- [15] G. Zhou, K. Liu, Y. Fan, M. Yuan, B. Liu, W. Liu, F. Shi, Y. Liu, W. Chen, J. Lopez, D. Zhuo, J. Zhao, Y. Tsao, X. Huang, Q. Zhang, Y. Cui, An aqueous inorganic polymer binder for high performance lithium-sulfur batteries with flame-retardant properties, *ACS Cent. Sci.* 4 (2018) 260–267, <https://doi.org/10.1021/acscentsci.7b00569>.
- [16] J. Sheng, Q. Zhang, M. Liu, Z. Han, C. Li, C. Sun, B. Chen, X. Zhong, L. Qiu, G. Zhou, Stabilized solid electrolyte interphase induced by ultrathin boron nitride membranes for safe lithium metal batteries, *Nano Lett.* 21 (2021) 8447–8454, <https://doi.org/10.1021/acs.nanolett.1c03106>.
- [17] D. Yeon, Y. Lee, M.H. Ryou, Y.M. Lee, New flame-retardant composite separators based on metal hydroxides for lithium-ion batteries, *Electrochim. Acta* 157 (2015) 282–289, <https://doi.org/10.1016/j.electacta.2015.01.078>.
- [18] J. Zhang, L. Yue, Q. Kong, Z. Liu, X. Zhou, C. Zhang, Q. Xu, B. Zhang, G. Ding, B. Qin, Y. Duan, Q. Wang, J. Yao, G. Cui, L. Chen, Sustainable, heat-resistant and flame-retardant cellulose-based composite separator for high-performance lithium ion battery, *Cellulose. Sci. Rep.* 4 (2014) 1–8, <https://doi.org/10.1038/srep03935>.
- [19] Q. Wang, B. Mao, S.I. Stoliarov, J. Sun, A review of lithium ion battery failure mechanisms and fire prevention strategies, *Prog. Energy Combust. Sci.* 73 (2019) 95–131, <https://doi.org/10.1016/j.pecs.2019.03.002>.
- [20] H. Liu, Z. Wei, W. He, J. Zhao, Thermal issues about li-ion batteries and recent progress in battery thermal management systems: a review, *Energy Convers. Manag.* 150 (2017) 304–330, <https://doi.org/10.1016/j.enconman.2017.08.016>.
- [21] W. Huo, Y. Qu, Effects of Bi1/2Na1/2TiO3 on the curie temperature and the PTC effects of BaTiO3-based positive temperature coefficient ceramics, *Sensors Actuators A Phys.* 128 (2006) 265–269, <https://doi.org/10.1016/j.sna.2006.01.022>.
- [22] S.W. Ding, G. Jia, J. Wang, Z.Y. He, Electrical properties of Y- and mn-doped BaTiO3-based PTC ceramics, *Ceram. Int.* 34 (2008) 2007–2010, <https://doi.org/10.1016/j.ceramint.2007.07.023>.
- [23] P.G. Balakrishnan, R. Ramesh, T. Prem Kumar, Safety mechanisms in lithium-ion batteries, *J. Power Sources* 155 (2006) 401–414, <https://doi.org/10.1016/j.jpowsour.2005.12.002>.
- [24] Z. Ling, F. Wang, X. Fang, X. Gao, Z. Zhang, A hybrid thermal management system for lithium ion batteries combining phase change materials with forced-air cooling, *Appl. Energy* 148 (2015) 403–409, <https://doi.org/10.1016/j.apenergy.2015.03.080>.
- [25] J. Weng, D. Ouyang, X. Yang, M. Chen, G. Zhang, J. Wang, Alleviation of thermal runaway propagation in thermal management modules using aerogel felt coupled with flame-retarded phase change material, *Energy Convers. Manag.* 200 (2019), 112071, <https://doi.org/10.1016/j.enconman.2019.112071>.
- [26] S.A. Khateeb, M.M. Farid, J.R. Selman, S. Al-Hallaj, Design and simulation of a lithium-ion battery with a phase change material thermal management system for an electric scooter, *J. Power Sources* 128 (2004) 292–307, <https://doi.org/10.1016/j.jpowsour.2003.09.070>.
- [27] Z. Rao, Q. Wang, C. Huang, Investigation of the thermal performance of phase change material/mini-channel coupled battery thermal management system, *Appl. Energy* 164 (2016) 659–669, <https://doi.org/10.1016/j.apenergy.2015.12.021>.
- [28] K. Liu, Y. Liu, D. Lin, A. Pei, Y. Cui, Materials for lithium-ion battery safety, *Sci. Adv.* 4 (2018), <https://doi.org/10.1126/sciadv.aas9820>.
- [29] D.R. MacNeil, J.R. Dahn, The reaction of charged cathodes with nonaqueous solvents and electrolytes: I. Li[sub 0.5]CoO[sub 2], *J. Electrochem. Soc.* 148 (2001) A1205, <https://doi.org/10.1149/1.1407245>.
- [30] R. Spotnitz, J. Franklin, Abuse behavior of high-power, lithium-ion cells, *J. Power Sources* 113 (2003) 81–100, [https://doi.org/10.1016/S0378-7753\(02\)00488-3](https://doi.org/10.1016/S0378-7753(02)00488-3).
- [31] X. Meng, S. Li, W. Fu, Y. Chen, Q. Duan, Q. Wang, Experimental study of intermittent spray cooling on suppression for lithium iron phosphate battery fires, *ETransportation* 11 (2022), 100142, <https://doi.org/10.1016/j.etrans.2021.100142>.
- [32] C. Tao, Q. Ye, C. Wang, Y. Qian, An experimental investigation on the burning behaviors of lithium ion batteries after different immersion times, *J. Clean. Prod.* 242 (2020), 118539, <https://doi.org/10.1016/j.jclepro.2019.118539>.
- [33] D. Ouyang, M. Chen, Q. Huang, J. Weng, Z. Wang, A review on the thermal hazards of the lithium-ion battery and the corresponding countermeasures, *Appl. Sci.* 9 (2019), <https://doi.org/10.3390/app9122483>.
- [34] M.N. Richard, J.R. Dahn, Accelerating rate calorimetry studies of the effect of binder type on the thermal stability of a lithiated mesocarbon microbead material in electrolyte, *J. Power Sources* 83 (1999) 71–74, [https://doi.org/10.1016/S0378-7753\(99\)00260-8](https://doi.org/10.1016/S0378-7753(99)00260-8).
- [35] R. Spotnitz, J. Franklin, Abuse behavior of high-power, lithium-ion cells, *J. Power Sources* 113 (2003) 81–100, [https://doi.org/10.1016/S0378-7753\(02\)00488-3](https://doi.org/10.1016/S0378-7753(02)00488-3).
- [36] M. Chen, D. Ouyang, J. Weng, J. Liu, J. Wang, Environmental pressure effects on thermal runaway and fire behaviors of lithium-ion battery with different cathodes and state of charge, *Process Saf. Environ. Prot.* 130 (2019) 250–256, <https://doi.org/10.1016/j.psep.2019.08.023>.
- [37] K. Liu, Y. Liu, D. Lin, A. Pei, Y. Cui, Materials for lithium-ion battery safety, *Sci. Adv.* (2018) 4, <https://doi.org/10.1126/sciadv.aas9820>.
- [38] G. Venugopal, Characterization of thermal cut-off mechanisms in prismatic lithium-ion batteries, *J. Power Sources* 101 (2001) 231–237, [https://doi.org/10.1016/S0378-7753\(01\)00782-0](https://doi.org/10.1016/S0378-7753(01)00782-0).
- [39] D.D. MacNeil, J.R. Dahn, The reaction of charged cathodes with nonaqueous solvents and electrolytes: I. Li[sub 0.5]CoO[sub 2], *J. Electrochem. Soc.* 148 (2001), A1205, <https://doi.org/10.1149/1.1407245>.
- [40] G. Zhong, B. Mao, C. Wang, L. Jiang, K. Xu, J. Sun, Thermal runaway and fire behavior investigation of lithium ion batteries using modified cone calorimeter, *J. Therm. Anal. Calorim.* 135 (2018) 2879–2889, <https://doi.org/10.1007/s10973-018-7599-7>.
- [41] H. Li, Q. Duan, C. Zhao, Z. Huang, Q. Wang, Experimental investigation on the thermal runaway and its propagation in the large format battery module with Li(Ni 1/3 co 1/3 Mn 1/3)O2 as cathode, *J. Hazard. Mater.* 375 (2019) 241–254, <https://doi.org/10.1016/j.jhazmat.2019.03.116>.
- [42] X. Feng, M. Fang, X. He, M. Ouyang, L. Lu, H. Wang, M. Zhang, Thermal runaway features of large format prismatic lithium ion battery using extended volume accelerating rate calorimetry, *J. Power Sources* 255 (2014) 294–301, <https://doi.org/10.1016/j.jpowsour.2014.01.005>.
- [43] X. Meng, K. Yang, M. Zhang, F. Gao, Y. Liu, Q. Duan, Q. Wang, Experimental study on combustion behavior and fire extinguishing of lithium iron phosphate battery, *J. Energy Storage* 30 (2020), 101532, <https://doi.org/10.1016/j.est.2020.101532>.
- [44] P. Russo, C. Di Bari, M. Mazzaro, A. De Rosa, I. Morriello, Effective fire extinguishing systems for lithium-ion battery, *Chem. Eng. Trans.* 67 (2018) 727–732, <https://doi.org/10.3303/CET1867122>.
- [45] L. Yi, Y. Dongxing, Z. Shaoyu, H. Qunming, L. Xin, W. Jianqiang, On the fire extinguishing tests of typical lithium-ion battery (In Chinese), *J. Saf. Environ.* 15 (2015) 120–125.
- [46] H. Rao, Z. Huang, H. Zhang, S. Xiao, Study of fire tests and fire safety measures on lithium ion battery used on ships, in: *ICTIS 2015 - 3rd Int. Conf. Transp. Inf. Safety, Proc.* 2015, pp. 865–870, <https://doi.org/10.1109/ICTIS.2015.7232158>.
- [47] L. Yujun, D. Qiangliang, L. Ke, C. Haodong, W. Qingsong, Experimental study on fire extinguishing of large-capacity lithium-ion batteries by various fire

- extinguishing agents(In Chinese), *Energy Storage Sci. Technol.* 7 (2018) 1105–1112, <https://doi.org/10.12028/j.issn.2095-4239.2018.0188>.
- [49] S. Yuan, C. Chang, S. Yan, P. Zhou, X. Qian, M. Yuan, K. Liu, A review of fire-extinguishing agent on suppressing lithium-ion batteries fire, *J. Energy Chem.* 62 (2021) 262–280, <https://doi.org/10.1016/j.jechem.2021.03.031>.
- [50] J. Zhigang, W.U. Hourong, S. Runquan, C. Xi, Research on the Technology of Fire Prevention and Extinction by direct injection of liquid carbon dioxide, *Phys. Numer. Simul. Geotech. Eng.* (2015) 36–42, <https://doi.org/10.5503/J.PNSGE.2015.21.006>.
- [51] S.S. Environments, Of fire sciences suppressant concentration needs for international space station environments, *J. Fire Sci.* 20 (2002) 391–399, <https://doi.org/10.1106/073490402031483>.
- [52] N. Saito, Y. Ogawa, Y. Saso, C. Liao, R. Sakei, Flame-extinguishing concentrations and peak concentrations of N₂, ar, CO₂ and their mixtures for hydrocarbon fuels, *Fire Saf. J.* 27 (1996) 185–200, [https://doi.org/10.1016/S0379-7112\(96\)00060-4](https://doi.org/10.1016/S0379-7112(96)00060-4).
- [53] J. Xu, P. Guo, Q. Duan, X. Yu, L. Zhang, Y. Liu, Q. Wang, Experimental study of the effectiveness of three kinds of extinguishing agents on suppressing lithium-ion battery fires, *Appl. Therm. Eng.* 171 (2020), <https://doi.org/10.1016/j.applthermaleng.2020.115076>.
- [54] Q. Wang, K. Li, Y. Wang, H. Chen, Q. Duan, J. Sun, The efficiency of dodecafluoro-2-methylpentan-3-one on suppressing the lithium ion battery fire, *J. Electrochem. Energy Convers. Storage* 15 (2018) 1–10, <https://doi.org/10.1115/1.4039418>.
- [55] Y. Li, D. Yu, S. Zhang, Q. Hu, X. Liu, J. Wang, On the fire extinguishing tests of typical Lithium-ion battery(In Chinese), *J. Saf. Environ.* 15 (2015) 120–125.
- [56] R. J. Si, D.Q. Liu, S.Q. Xue, Experimental study on fire and explosion suppression of self-ignition of lithium ion battery, *Procedia Eng.* 211 (2018) 629–634, <https://doi.org/10.1016/j.proeng.2017.12.057>.
- [57] Q. Wang, G. Shao, Q. Duan, M. Chen, Y. Li, K. Wu, B. Liu, P. Peng, J. Sun, The efficiency of heptafluoropropane fire extinguishing agent on suppressing the lithium titanate battery fire, *Fire Technol.* 52 (2016) 387–396, <https://doi.org/10.1007/s10694-015-0531-9>.
- [58] J.L. Pagliaro, G.T. Linteris, Hydrocarbon flame inhibition by C6F12O (Novoc 1230): unstretched burning velocity measurements and predictions, *Fire Saf. J.* 87 (2017) 10–17, <https://doi.org/10.1016/j.firesaf.2016.11.002>.
- [59] A.O. Said, S.I. Stoliarov, Analysis of effectiveness of suppression of lithium ion battery fires with a clean agent, *Fire Saf. J.* 121 (2021), 103296, <https://doi.org/10.1016/j.firesaf.2021.103296>.
- [60] NFPA, *Standard on Water Mist Fire Protection Systems*, 2019.
- [61] Q. Wang, Y. Wang, H. Chen, The efficiency of dodecafluoro- 2-Methylpentan-3-one on suppressing the lithium ion battery fire, *J. Electrochem. Energy Convers. Storage* 15 (2019) 1–10, <https://doi.org/10.1115/1.4039418>.
- [62] Y. Liu, Q. Duan, J. Xu, H. Chen, W. Lu, Q. Wang, Experimental study on the efficiency of dodecafluoro-2-methylpentan-3-one on suppressing lithium-ion battery fires, *RSC Adv.* 8 (2018) 42223–42232, <https://doi.org/10.1039/c8ra08908f>.
- [64] Y. Liu, Q. Duan, J. Xu, H. Li, J. Sun, Q. Wang, Experimental study on a novel safety strategy of lithium-ion battery integrating fire suppression and rapid cooling, *J. Energy Storage* 28 (2020) 101–185, <https://doi.org/10.1016/j.est.2019.101185>.
- [65] J. Zhao, Y. Cheng, S. Lu, A comparative study on the thermal runaway inhibition of 18650 lithium-ion batteries by different fire extinguishing agents, *IScience* 24 (2021), 102854, <https://doi.org/10.1016/j.isci.2021.102854>.
- [66] T. Liu, C. Tao, X. Wang, Cooling control effect of water mist on thermal runaway propagation in lithium ion battery modules, *Appl. Energy* 267 (2020), 115087, <https://doi.org/10.1016/j.apenergy.2020.115087>.
- [67] T. Liu, Y. Liu, X. Wang, X. Kong, G. Li, Cooling control of thermally-induced thermal runaway in 18,650 lithium ion battery with water mist, *Energy Convers. Manag.* 199 (2019), 115087, <https://doi.org/10.1016/j.enconman.2019.111969>.
- [68] L. Zhang, Q. Duan, Y. Liu, J. Xu, J. Sun, H. Xiao, Experimental investigation of water spray on suppressing lithium-ion battery fires, *Fire Saf. J.* (2020), 103117, <https://doi.org/10.1016/j.firesaf.2020.103117>.
- [69] Y. Huang, Y. Wu, B. Liu, Experimental investigation into the use of emergency spray on suppression of battery thermal runaway, *J. Energy Storage* 38 (2021), 102546, <https://doi.org/10.1016/j.est.2021.102546>.
- [70] L. Zhang, Q. Duan, X. Meng, K. Jin, J. Xu, J. Sun, Q. Wang, Experimental investigation on intermittent spray cooling and toxic hazards of lithium-ion battery thermal runaway, *Energy Convers. Manag.* 252 (2022), 115091, <https://doi.org/10.1016/j.enconman.2021.115091>.
- [71] T. Liu, J. Hu, C. Tao, X. Zhu, X. Wang, Effect of parallel connection on 18650-type lithium ion battery thermal runaway propagation and active cooling prevention with water mist, *Appl. Therm. Eng.* 184 (2021), 116291, <https://doi.org/10.1016/j.applthermaleng.2020.116291>.
- [72] T. Liu, J. Hu, Q. Tang, X. Zhu, X. Wang, Mitigating overcharge induced thermal runaway of large format lithium ion battery with water mist, *Appl. Therm. Eng.* 197 (2021), 117402, <https://doi.org/10.1016/j.applthermaleng.2021.117402>.
- [73] Z. Qingsong, C. Xiangjing, B. Wei, C. Wenjie, Experimental study on suppressing thermal control of Lithium-ion batteries with additive water mist(In Chinese), *Sci. Technol. Eng.* 18 (2018) 372–376, <https://doi.org/10.1201/9781420072365.ch1>.
- [74] Z. Qingsong, L. Xingna, C. Xiangjing, B. Wei, Method of screening fine water mist additive based on temperature drop index of lithium battery(In Chinese), *J. Beijing Univ. Aeronaut. Astronaut.* 46 (2019) 1073–1079.
- [75] Z. Qingsong, C. Xiangjing, B.A.I. Wei, Study on optimum concentration of additives in water mist for suppression of lithium battery fire(In Chinese), *J. Saf. Sci. Technol.* 14 (2018) 43–50.
- [76] Z. Zhengl, Y. Jianhua, Z. Ping, Z. Qin, Z. Shunbing, Fire extinguishing test of power lithium ion battery by water mist with additive(In Chinese), *Fire Sci. Technol.* 38 (2019) 512–516.
- [77] Xun, Li, Shunbing, Zhu, Weiqiang, Zhuang, Xuotong, Hao, Experimental study on the suppression of fire in lithium iron phosphate battery with additive water mist, in: 2018 IEEE Int.Conf. Saf. Prod. Informatiz, IEEE, 2018, pp. 53–56, <https://doi.org/10.1109/IICSPI.2018.8690326>.
- [78] M. Egelhaaf, D. Kress, D. Wolpert, T. Lange, Fire fighting of li-ion traction battery, *SAE Int. J. Alt. Powertrans.* 2 (2013) 37–48.
- [79] W.T. Luo, S.B. Zhu, J.H. Gong, Z. Zhou, Research and development of fire extinguishing technology for power lithium batteries, *Procedia Eng.* 211 (2018) 531–537, <https://doi.org/10.1016/j.proeng.2017.12.045>.
- [80] Z. Qingsong, C. Xiangjing, B. Wei, Analysis on fire suppression performance of water mist compound additive on lithium battery fire(In Chinese), *Fire Sci. Technol.* 37 (2018) 1211–1214.
- [81] Z. Mingxing, Z. Shunbing, L. Weitao, Study on fire suppression of lithium batteries with surfactant water mist, *Fire Sci. Technol.* 37 (2018) 799–803.
- [82] M.X. Zhu, S.B. Zhu, J.H. Gong, Z. Zhou, Experimental study on fire and explosion characteristics of power lithium batteries with surfactant water mist, *Procedia Eng.* 211 (2018) 1083–1090, <https://doi.org/10.1016/j.proeng.2017.12.113>.
- [83] Y. Zhou, Z. Wang, H. Gao, X. Wan, H. Qiu, J. Zhang, J. Di, Inhibitory effect of water mist containing composite additives on thermally induced jet fire in lithium-ion batteries, *J. Therm. Anal. Calorim.* (2021), <https://doi.org/10.1007/s10973-021-10673-x>.
- [84] T. Maloney, U.S.D. of T.F.A. Administration, *Extinguishment of Lithium-Ion and Lithium-Metal Battery Fires*, 2017.
- [85] A.W. Golubkov, D. Fuchs, J. Wagner, H. Wiltsche, C. Stangl, G. Fauler, G. Voitc, A. Thaler, V. Hacker, Thermal-runaway experiments on consumer Li-ion batteries with metal-oxide and olivin-type cathodes, *RSC Adv.* 4 (2014) 3633–3642, <https://doi.org/10.1039/c3ra45748f>.
- [86] A.R. Baird, E.J. Archibald, K.C. Marr, O.A. Ezekoye, Explosion hazards from lithium-ion battery vent gas, *J. Power Sources* 446 (2020), 227257, <https://doi.org/10.1016/j.jpowsour.2019.227257>.
- [87] L. Zhigang, K. Andrew, Review of water mist fire suppression systems - fundamental studies, *J. Fire Prot. Eng.* 10 (2000) 32–50, <https://doi.org/10.1177/104239159901000303>.
- [88] Project BLUE BATTERY, Part II : Assessment of Existing Fire Protection Strategies and Recommendation for Future Work, 2017.
- [89] Z. Daoliang, F. Tingyong, L. Feng, Experimental research on low pressure water mist system in extinguishing oil fires with F-500(In Chinese), *J. Saf. Sci. Technol.* 6 (2010) 9–14.
- [90] HCT(Hazard Control Technologies Inc.), *Material Safety Data Sheet F-500 Multi-Purpose Encapsulator Agent*, 2018.
- [91] P. Mukerjee, Odd-even alternation in the chain length variation of micellar properties, *Kolloid Z. Z. Polym.* 236 (1970) 76–79.